BNL-101857-2014-TECH
AD/RHIC/RD/75;BNL-101857-2013-IR

Closed Orbit Calculations at AGS and Extraction Beam Parameters at H13

N. Tsoupas

October 1994

Collider Accelerator Department
Brookhaven National Laboratory

U.S. Department of Energy
USDOE Office of Science (SC)

DISCLAIMER

AD/RHIC/RD–75

RHIC PROJECT

Brookhaven National Laboratory

Closed Orbit Calculations at AGS and Extraction Beam Parameters at H13

N. Tsoupas, H. W. Foelsche, J. Claus and R. Thern

October 1994

CLOSED ORBIT CALCULATIONS AT AGS AND EXTRACTION BEAM PARAMETERS AT H13.

N. Tsoupas, H.W. Foelsche, J. Claus and R. Thern

Introduction

A critical step in the filling procedure of RHIC is the extraction of the beam from the AGS. Because the possibilities for the correction of random variations in this process are rather limited, it is important that it repeat from cycle to cycle to within small tolerances. Its dependence on the various operating parameters should be weak, so that unavoidable changes do not affect it too drastically and servo systems can be relied upon to keep them under control. Extraction involves the following sequence of events: the closed orbit on which the beam circulates is adiabatically contracted or expanded to become the extraction closed orbit, defined in radial location relative to the machine structure to within a few 0.01mm, by means of a BPM. That orbit is adiabatically distorted by two superimposed bumps that drive it into the aperture of an extraction kicker, and close to, but still on the machine side of the septum of a septum magnet. Excitation of the extraction kicker drives it to the other side of the septum, where the field drives it, via the stray fields of some of the main magnets of the ring, into the transfer line to RHIC. The desired coordinates in phase space (x, x', y, y') of this no-longer-closed orbit at the entrance of the transfer line are fixed relative to the AGS coordinate system.

The system is inherently dispersive at that entrance, but the tolerance of the particle momentum, set by the acceptable degree of blowup in longitudinal phase space and/or the acceptable strength of a longitudinal damper in RHIC, is sufficiently small to make that factor disregardable for the present purpose. Dilution of the beam emittance is then minimized if the focusing parameters at the entrance of the transfer line are matched to those at the exit of the extraction system. The transfer line can be tuned (within limits) to provide such matches but the extraction system must be stable enough to maintain them. These factors are all affected by the operating conditions in the AGS at extraction time. The choice of extraction momentum, extraction closed orbit, bump magnitudes, radial locations of kicker and septum magnets, betatron tunes, chromaticities, all play their roles and can all be adjusted to provide an optimum system. They are also affected by less controllable factors

such as, the actual geometry of the AGS, the non-linearities of its guide field, and its stray field in the regions where the extracted beam passes. The present note describes calculations done to provide information for the final design of the transfer line and to initiate the search for optimum extraction.

Procedure to Calculate the Beam Parameters at the Extraction Point H13

The first section of the beam transfer line from AGS to RHIC (Ref.1) is the "U-Line". The beam optics of the U-Line requires a reliable specification of the beam parameters at its starting point, the AGS extraction point H13 (see appendix A1 for definition). Beam parameters at the AGS extraction point H13 had been calculated (Ref. 2), and also measured experimentally (Ref. 3) for a fast beam extraction system which is described in Ref. 2. Recently, a new fast beam extraction system ("NewFEB" Ref. 6) has been adopted for the AGS; therefore a new set of calculations was required to determine the beam parameters at H13.

These calculations were performed using the computer code BEAM (ref. 4). At this time the BEAM code offers the most reliable method of tracking the extracted beam through the AGS fringe field. For purposes of these calculations, this code was modified in two ways to enable it to read and then use the experimentally-measured magnetic field maps of the AGS magnets (ref. 5) and to provide for the simulation of the extraction bumps of the New Fast Beam Extraction (NewFEB) system (Ref. 6). Once the computer code was modified (see more detailed descriptions in Appendices A2 and A3) the calculations were carried out in two steps:

a) The closed orbit calculations in the AGS.

b) The beam extraction calculations.

In the first step (a), which is described in more detail in a later section, the BEAM code calculates the closed particle orbit of the central ray by numerical integration of the differential equation of motion using the experimentally-measured magnetic field maps described in Appendix A2, and a Runge Kuta integration procedure. The closed orbit calculations include the effect of the new extraction bumps (Appendix A3 and Ref.6). The results of the closed orbit calculations provide all the necessary information (central and off momentum orbit trajectories as well as beta-functions) required for the extraction calculations in step (b). In the second step (b), also to be described in more detail in a separate section below, the tracking of the extracted beam starts from a particular azimuthal location in the AGS ring (we have chosen the center of the straight section G09). The bumped closed

orbit experiences a "kick" by the kicker (located in the straight section G10) which breaks the closed orbit, and the central particle follows a new orbit which takes it to the septum magnet at H10 (located downstream at the straight section H10) which then deflects the particle out of the AGS through the fringing field of the H11, H12, and H13 AGS magnets, to the extraction point H13. In step (b) the code also calculates the beam trajectories for the central and off momentum particles from the starting point G09 to the extraction point H13; from this information the dispersion function along the extraction trajectory can be calculated. In addition the code calculates the R-matrix (2x2 first order transfer matrix) between the above two points (G09 to H13) and from the knowledge of the beam parameters at the point G09 (calculated in step a) we can calculate all beam parameters at the location of the extraction point H13.

Closed Orbit Calculations

The closed orbit calculations for the AGS were performed with the modified computer code BEAM (ref. 4, Appendices A2 and A3). Details and results of these calculations are presented in the following two sections. Since only two sets of field maps are available, one for open magnets (type A), and one for closed magnets (type C), we assumed that all magnets of a type have identical field maps, we also assumed perfect superperiodicity in the locations/orientations of the magnets in the ring. Together these assumptions generate perfect superperiodicity in the calculations.

Closed Orbit Results for the "Bare" AGS Machine.

The Closed Orbit results for a "bare" AGS machine (only the AGS main magnets are energized) are not required for the calculation of the beam parameters at the extraction point H13. However, we feel that we should present these results in order to provide information for comparison with the corresponding results of other codes. Using BEAM we varied the particle momentum in order to position the central particle orbit at the Optimum Closed Orbit (OCO) defined in ref. 7. During these closed orbit calculations we observed that the computed bending angles for the types A and B magnets were slightly different from the nominal ones (27.96 mrad and 23.5 mrad respectively) and this caused the central orbit to deviate slightly from the OCO. To minimize this deviation we multiply the magnitudes of the field and the gradient of all the C-type magnets by a factor 0.9985. After this correction the central ray with momentum p_0=29.2305 GeV/c coincided with the OCO to within 0.1

mm everywhere.[1] In Fig. 1 the small squares of the middle curve represent the deviation of the closed orbit from the OCO midway at the various straight sections of the AGS ring for the momentum p_0. The curve joining the small squares is to guide the eye. Similarly the top and bottom curves of Fig.1 show deviations of closed orbits from the OCO for the off momentum trajectories $p_+ = p_0 (1 + 0.0005)$ (top) and $p_- = p_0 (1 - 0.0005)$ (bottom). The calculated horizontal and vertical beta functions corresponding to the OCO appear in Fig 2. In Fig. 3 the small squares represent the value of the dispersion function at the

various straight sections of the AGS ring. In order to calculate the value of the dispersion function shown in Fig.3 the code calculates the trajectories for three different momenta p_0, $p_+ = p_0 (1 + 0.0005)$, $p_- = p_0 (1 - 0.0005)$, and the value of the dispersion function at a given point along the central ray is calculated from the formula $D = \Delta r/(2 \Delta p/p)$ where Δr is the radial distance of the two off momentum particles and $\Delta p/p = 0.0005$. (The dispersion function is the differential $dx/(dp/p)$ therefore independent of higher order fields (sextupoles and higher), the one given here is an approximation). The list of the most important parameters of the OCO for a bare machine is given in the first column of Table I. The layout of the AGS magnets used in the BEAM code, corresponds to the optimum closed orbit as described in ref. 8. Therefore all the calculations are based on the theoretical layout of the machine and not on the actual locations of the AGS magnets. The results of the BEAM code calculations for the "bare machine" agree very closely with results obtained with a MAD code simulation of the AGS.

Optimum Closed Orbit With Bumps and Extraction

The extraction bumps deflect the central beam orbit into the aperture of the kicker, centered on the middle of the straight section G10, and also provide the correct displacement of the central orbit at the middle of the straight section H10 where the septum magnet is located. The relative strengths of the bumps can be adjusted to minimize any small oscillations (residuals) of the central orbit relative to the OCO in the regions outside the bumps (straight section I13 to F08) regardless of the betatron tunes. These residuals are caused because the back-leg windings that generate the bumps,

[1]In the rest of the report particle with momentum $p_0 = 29.2305$ GeV/c will be considered as the particle which best describes the OCO.

are distributed in phase relationships that are slightly different from the ideal one required for perfect cancellation. The strengths of the bumps are adjusted so that the specified central orbit displacements, 6.1 cm at G10 and 4.78 cm at H10, are obtained. After the equilibrium orbit is established the kicker at G10 is turned on in order to break the equilibrium orbit, and deflect it into the Septum magnet located at H10.

In the remainder of this section we describe the procedure used to establish the equilibrium orbit and to extract the beam from AGS.

1) Run the BEAM code in the "closed orbit calculation mode" with the extraction bumps on. (The momentum of the central orbit particle is $p_0 = 29.2305$ GeV/c, and particles with this momentum circulated on the OCO). The code calculates the strength of the bumps required to achieve the correct displacement at G10 and H10 while minimizing the residuals outside the region of the bumps.

2) With the bump strengths calculated in step (1), we run BEAM code in the "closed orbit calculation mode" for three momenta p_0, p_+, p_- and record the corresponding beam parameters (H/V beta's and alpha's) and the coordinates (radial excursion and slope with respect to the central orbit at G09 which is the straight section prior to the kicker at G10). This information will be used in step (3) below to extract the beam from the machine. In the closed orbit calculation above we have chosen $\pm 0.05\%$ momentum[2] deviations for the off momentum particles p_+ and p_-, and an integration step equal to 1 inch[3], required by the BEAM code. In addition to the above results obtained in this step, additional information (dispersion as well as H/V betatron functions) of the central orbit is also obtained.

---

[2]The momentum spread of 0.05% is a realistic estimate of the beam in AGS.

[3]For the momentum spread chosen, the step size of 1" is good compromise between computer time and accuracy of the results. Smaller integration steps like 0.5"or 0.25"yield almost identical results. Step sizes larger than 4" introduce an integration error which is larger than the effect produced by the momentum spread of 0.05%.

3) Using the beam coordinates at G09 obtained above, we run BEAM to trace rays with momenta p_0, p_+, and p_-, starting at the G09 and ending at extraction point H13. The kicker at G10 is on and we adjust its strength so that the central orbit passes through a specified point at H10 (7.55 cm in the OCO system). This displacement places it well within the aperture of the septum magnet. Subsequently we adjust the strength of the septum magnet so that the extracted central orbit passes through the extraction point at H13. The magnetic strength of the bumps is kept the same as calculated in step (1). The results we obtain in this step are: a) the trajectories of the three orbits above (p_0, p_+, p_-) in the coordinate system specified by BEAM. Thus we have knowledge of the direction of the central orbit when it passes through the extraction point at H13. From the trajectories of the off momentum particles (p_+ and p_-) we calculate the dispersion along the central orbit as described earlier. b) The R-matrix (2x2 first order transfer function) of the beam line starting from the G09 to the extraction point at H13. Knowledge of the R-matrix and the beam parameters at G09 is sufficient to calculate the beam parameters at H13. Fig. 4 shows the displacement of the closed orbit (in OCO system) along the ring, from the straight sections E10 to J10 (labeled SS90 and SS190 on the graphs). In this figure, the magnets with bump coils are indicated with arrows. Table I shows the relative strengths of the bumps required to achieve the equilibrium orbit shown in Figure 4. Figure 5 shows the calculated horizontal/vertical beta-functions. Figure 6 shows the dispersion function, calculated using the method described in the previous section.

Results

In this section we discuss the results obtained from the closed orbit calculations and their corresponding beam parameters at the extraction point H13. In all the closed orbit calculations we adjust the bumps in order to obtain not only the correct central ray displacement at the straight sections G10 and H10 but also zero residuals (NO/RES in table I) in the regions outside the bumps unless we state otherwise (W/RES in table I). The results are tabulated in the various columns of table I and each column corresponds to a particular set up of the extraction process. The first part of the table "Extraction at H13" tabulates the beam parameters at H13, the strengths of the G10 kicker

and H10 septum magnet in mrad, the slope x', the dispersion η_h and the angular dispersion η_h' of the central trajectory at the straight section H10. In all extraction processes the central trajectory meets the extraction point H13 (44.6 cm from the OCO) with a slope 69.54 mrad with respect to the oco in straight section H13. The second part of the table tabulates some of the parameters associated with the various orbits. The dispersion and the angular dispersion quantities presented in table I, are in reference to the coordinate system used in BEAM. The signs of these quantities may have to be changed if they are used as input parameters in codes (MAD or TRANSPORT) whose sign convention may be different from that of Beam. The horizontal (Ξ_h) and vertical (Ξ_v) chromaticities are calculated using the formula $= (\nu_+ - \nu_-) / dp/p_0$, where ν_+ and ν_- are the tunes of the off momentum closed orbits. The strengths of the bumps that produce the equilibrium orbit for a given set up of the AGS, are given in Table I. A description of the physical arrangement of the bumps, is given in Appendix A3 and Table A3.I. A number of closed orbits for different AGS setups are described below:

1. Closed orbit calculations (Bare machine, no extraction bumps).
   The relevant results from the closed orbit calculations for the bare AGS appear in column 1 of table I. The calculations have been performed for one super period of the AGS machine and it is understood that the bumps are off. Fig. 1, 2 and 3 show the location of the closed orbit in the OCO system, the horizontal and vertical beta functions, and the dispersion functions respectively, at the midpoint of each straight section of a super period of the AGS machine.

2. Closed orbit calculations (Extraction bumps are on, NO/RES).
   These calculations pertain to the extraction closed orbit, i.e., main extraction bumps are activated and adjusted to give the orbit the proper displacements from the OCO at the centers of the G10 and H10 straight sections and to eliminate the residual oscillations (NO/RES) outside the bumps region (see Fig. 4). To achieve this, the power supplies 1a and 1b of the first bump as well as the power supplies 2a and 2b of the second were adjusted independently of each other. Table I (column 3) shows the relative strength of

the bumps. The beam parameters at the extraction point H13 appear on the first six lines of the column 3. This extraction process is simple, however the horizontal tune is close to a half integer ($\nu_h = 8.6$), this may be a less desirable operating point for the AGS.

3. Closed orbit calculations (Extraction bumps are on, W/RES).
In this extraction process the main bumps were adjusted to achieve the correct displacement of the closed orbit at the G10 and H10 midpoints without regard for residual oscillations outside the main bumps. The adjustment of the bumps in this extraction process consisted of varying the power supplies 1a and 1b not independently but in conjunction. Similarly the power supplies 2a and 2b were varied in conjunction. The relative strengths of the power supplies appear on column 4 of table I. Fig. 7 shows the equilibrium orbit for this extraction process with the residual oscillations of the closed orbit shown clearly in the region outside the bumps. The beam parameters at the extraction point H13 are almost identical to the ones of the extraction process 2 above, except for the dispersion and angular dispersion values. Comparison of the results in section 2 and 3 shows that the strengths of the extraction bumps have a definite effect on the dispersion and angular dispersion at the extraction point H13. As in the extraction process 2 above, the horizontal tune of the machine is close to a half integer (ν_h=8.6).

4. Closed orbit calculations (Extraction bumps, High field Quads, NO/RES).
The horizontal and vertical tunes of the AGS can be controlled with the high field quadrupoles. These were adjusted so that the horizontal and vertical tunes were 8.78 and 8.72 respectively. As in case 2, the strength of the bumps was adjusted to achieve a central closed orbit without residual oscillations and the correct displacements at the center of G10 and H10 (see Fig. 8). The relative strength of the bumps and the beam parameters at the extraction point H13 appear in table I.

5. Closed orbit calculations (Extraction bumps, High field Quads,W/RES).
This extraction process is similar to the extraction process 3 above, except that the

bumps were adjusted to provide only the correct excursions at the G10 and H10 centers without regard for the residuals outside the bump region. Fig. 9 shows the excursion of the equilibrium orbit for $\nu_h = 8.78, \nu_v = 8.72$. The large residuals of this orbit are shown in Fig. 8, are mainly due to the high field quadrupoles at F17, G03, G17, H03, H17, and I03, which are located in the bump region. The corresponding beam parameters at H13 are shown in table I.

Summary and Conclusions

This report describes a method for calculating the beam parameters of the AGS at the extraction point H13 (see Table I). The method makes use of the experimentally measured fields of the AGS magnets, and accounts for the fringing fields through which the beam passes during the extraction process. The calculations assume that all magnets of a type have identical magnetic fields and are located according to design. For the extraction processes studied, the existing bumps are sufficient to generate the proper equilibrium orbit, with or without residuals outside of the bump region and there is no need of trim bumps. The required horizontal and vertical tunes can be achieved within the range of the highfield quadrupoles. If there is a need to change the horizontal and vertical chromaticity, the AGS sextupoles must be employed. This may require trim bumps (ref. 10) in order to minimize the residuals. The extent to which the horizontal and vertical chromaticities of the AGS can be varied within the strength limits of the available sextupoles while minimizing the residuals may be the subject of a new study.

ACKNOWLEDGEMENTS

One of the authors would like to thank C.J. Gardner of AGS for making available the latest version of the BEAM code, as well as for all his personal notes regarding the code; the authors also wish to thank E. Bleser, H. Brown, Y.Y. Lee, M. Tanaka, W. T. Weng, all of AGS, for their valuable comments in all the meetings held regarding the simulation of the beam extraction from AGS using the BEAM code. Many thanks to M. Campbell for her patience and the excellent job in preparing this report.

REFERENCES

Ref. 1 J. Claus and H. Foelsche, "Beam Transfer from AGS to RHIC", RHIC Technical Note 47

Ref. 2 W. T. Weng, "The New Fast Extraction System", BNL-51310, September 15, 1980

W. T. Weng, "Momentum Dispersion of AGS Fast Extracted Beam", BNL-24658, April 25, 1978

Ref. 3 J. Ryan, R. Thern, "Measurement of the Twiss parameters and Emittance in the U-Line", AGS Studies Report 193

Ref. 4 C. J. Gardner, "The New BEAM Program", Accelerator Division Tech. Note (Draft)

G. H. Morgan, "Fortran IV Version of Beam the AGS Orbit Computing Program", AGS Internal Report

E. D. Courant, "Computations of AGS Orbits with 704 Computer", ADD Internal Report EDC-36

Ref. 5 R. Thern, Experimental Magnetic Field Maps of the AGS Dipole Magnets, (Private Communication)

Ref. 6 M. Tanaka, "The New Fast Extraction System [NewFEB] at the AGS", AGS/AD/Tech. Note 347

Ref. 7 E. Bleser, "Where are the AGS Magnets?", Accelerator Division Technical Note 215

Ref. 8 E. Bleser, "The Optimum Central Orbit in the AGS", Accelerator Division Technical Note 217

Ref. 9 Vector Fields Inc.

Ref. 10 Hugh Brown, (BNL-AGS Dept.), Private communication

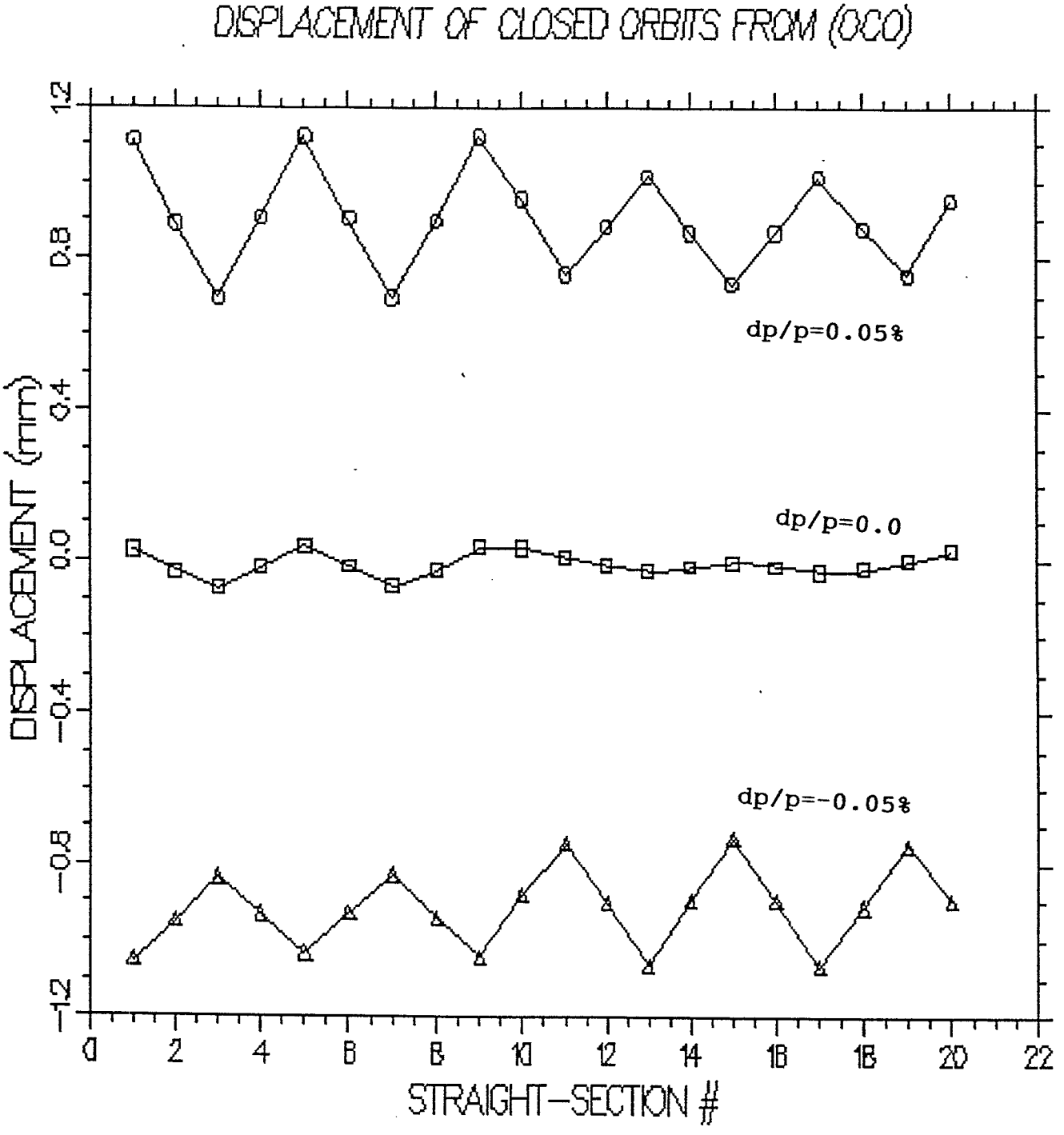

Fig. 1 Displacements of closed central orbit (in the OCO system) at the midpoints of the straight sections of an AGS superperiod, for three different particle momenta:

$$p_0 = 29.2305\ GeV/c,\ p_+ = p_0 + \delta p/p,\ p_- = p_0 - \delta p/p$$

The values of the displacement are represented by the small squares. The curve through the squares is to guide the eye.

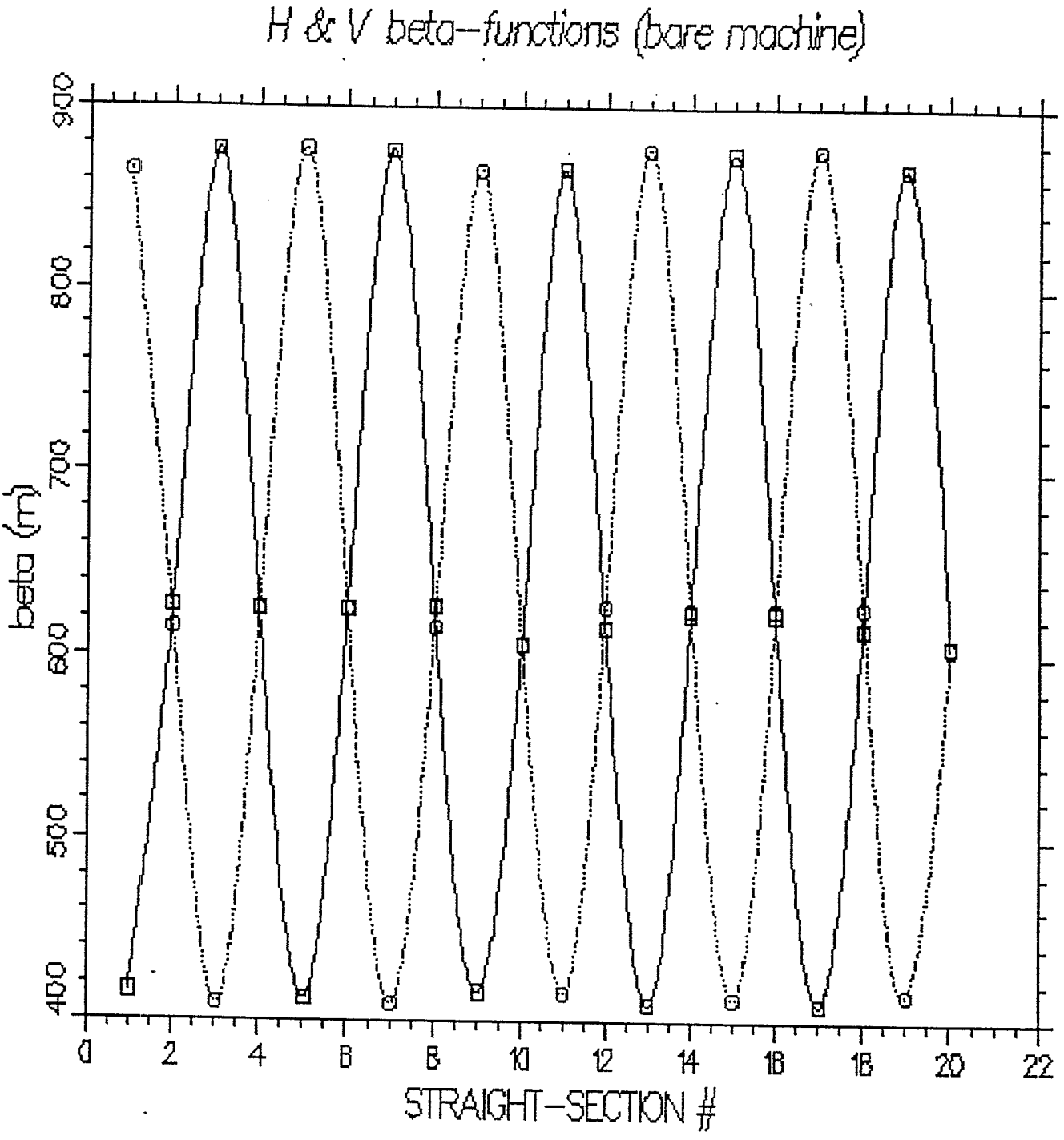

Fig. 2 Horizontal (open squares on the solid line) and vertical (open circles on the broken line) beta functions in the straight sections of a superperiod of the bare AGS. The beta functions correspond to the Optimum Closed Orbit (OCO). The curves are to guide the eye.

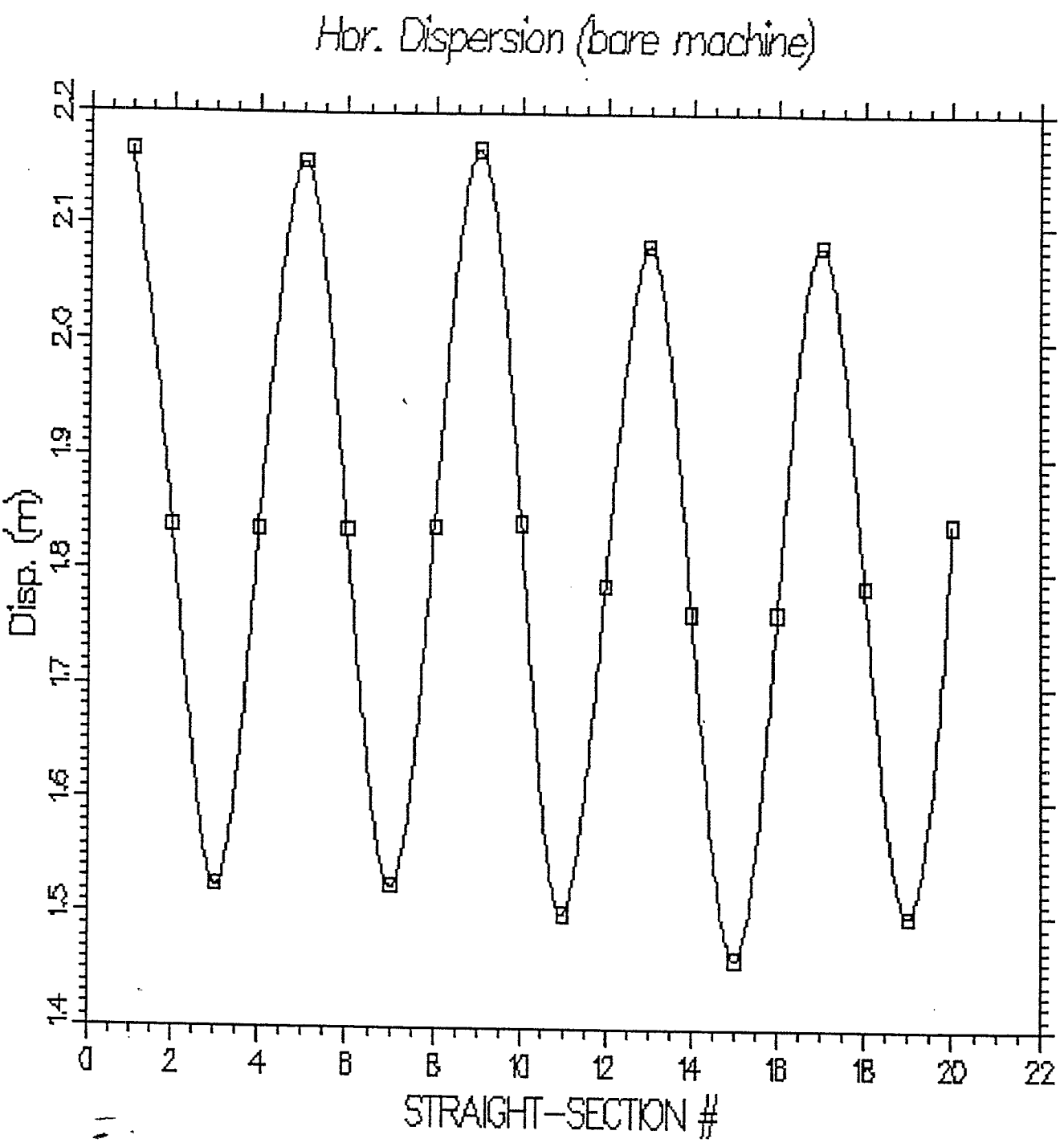

Fig. 3 Values of the dispersion function (open squares) in the straight sections of a superperiod of the bare AGS machine. The curve is to guide the line.

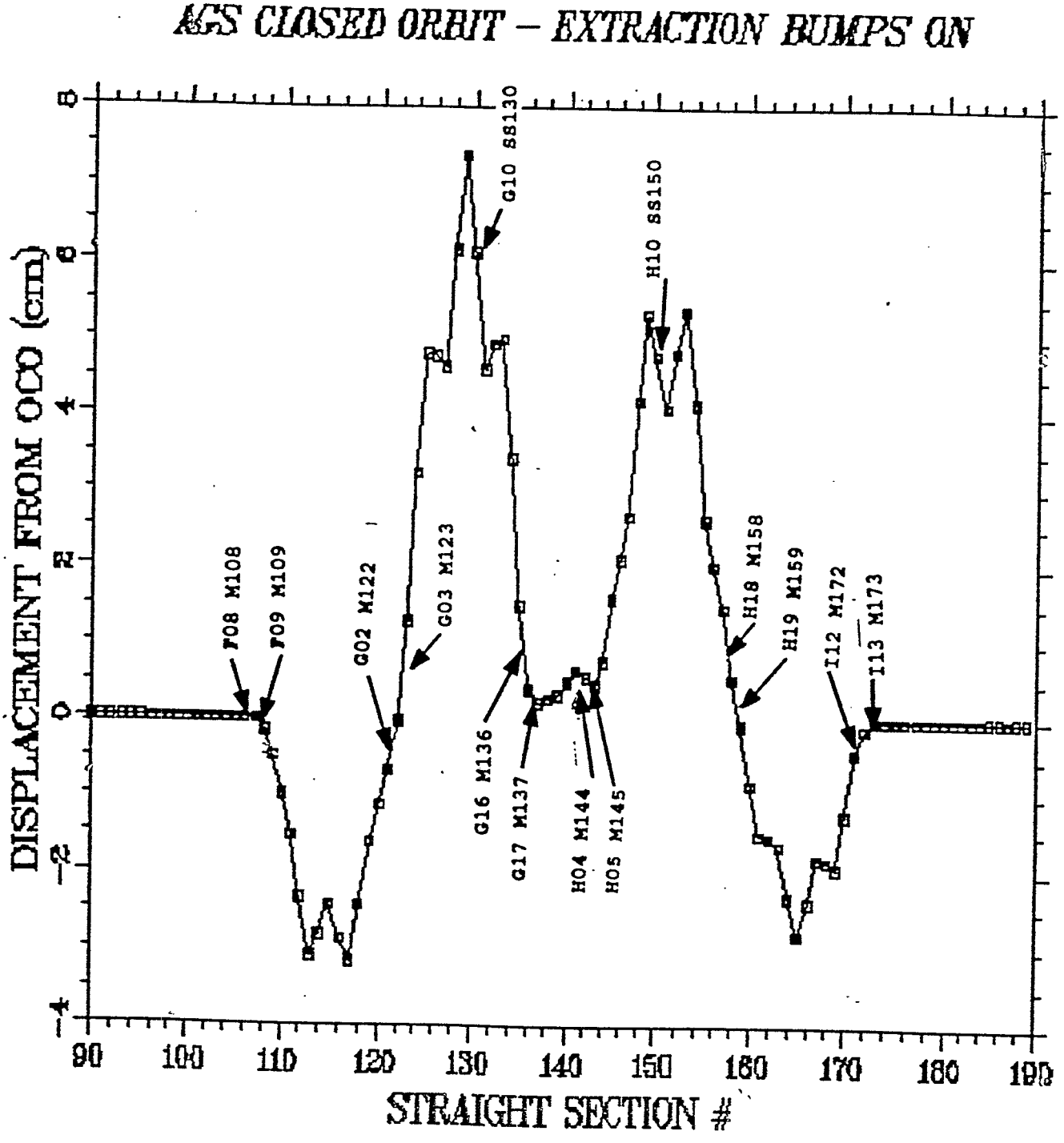

Fig. 4 Displacements of the central orbit (in OCO system) in the straight sections E10 (SS90) to J10 (SS190) of the AGS. The location of the extraction bump coils is indicated by arrows. The strengths of the bumps are adjusted such that the closed orbit coincides with the OCO outside the bump region (F08 to I13). The curve is to guide the eye.

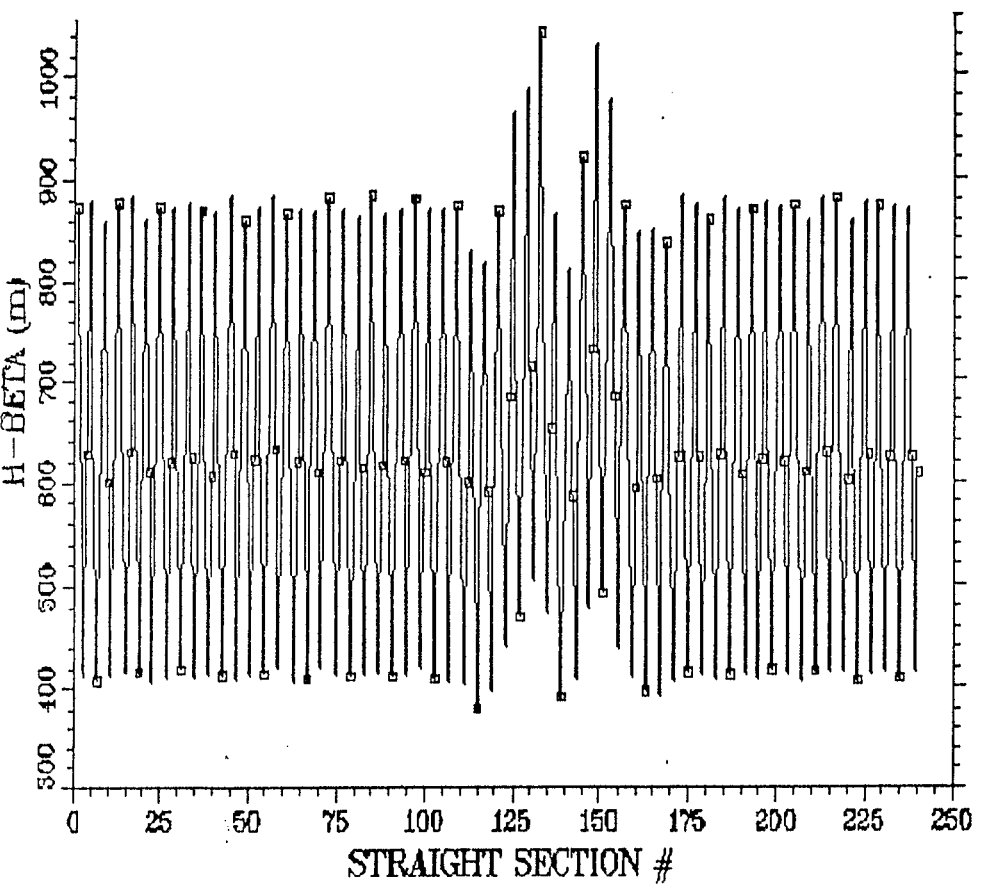

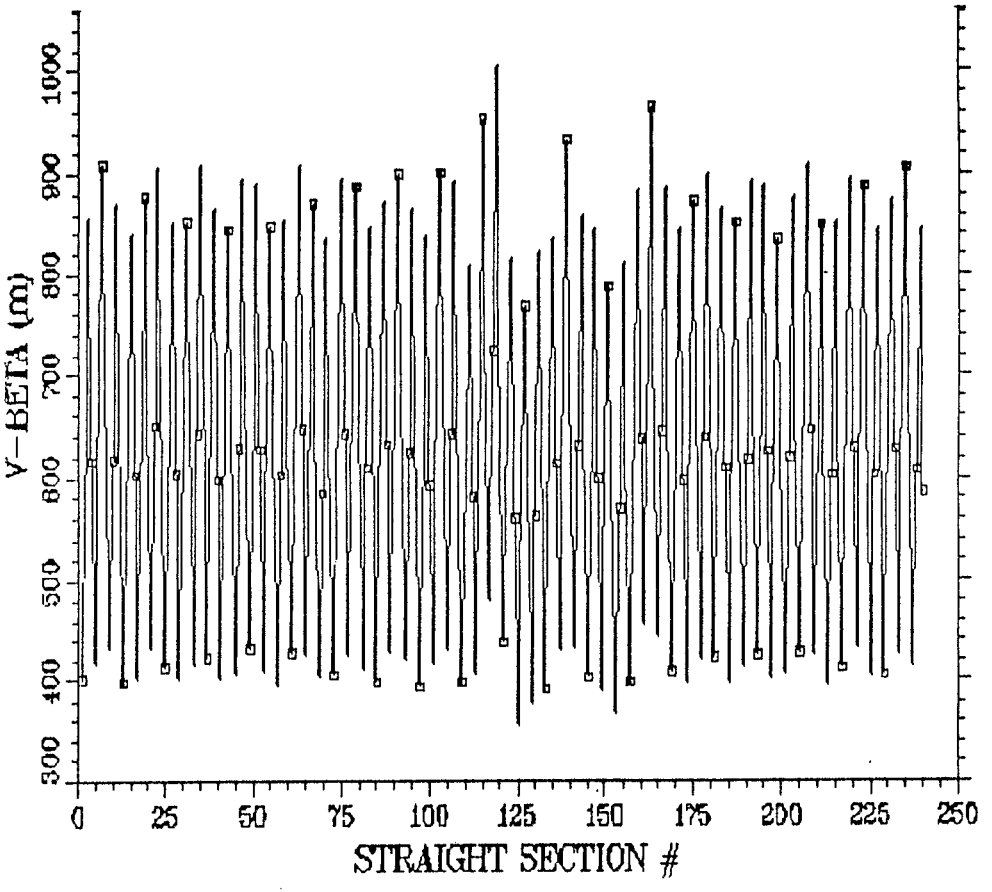

Fig. 5 Horizontal (left) and vertical (right) beta functions at the straight sections of the AGS machine. With the bumps energized (see Fig. 4). The line between the small squares is to guide the eye.

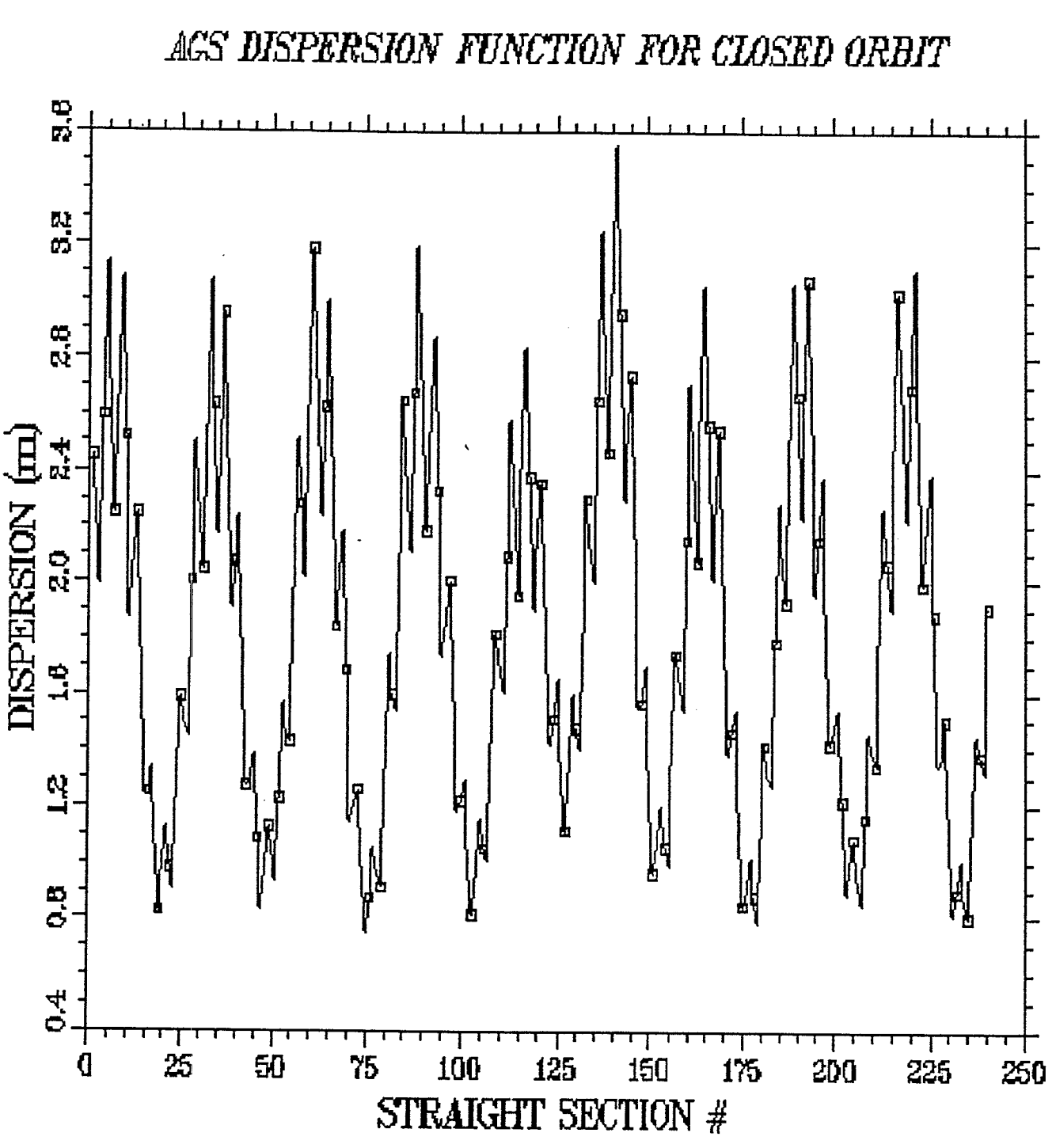

Fig. 6 Magnitude of the dispersion function in the straight sections of the AGS. The line passes through the points and is to guide the eye.

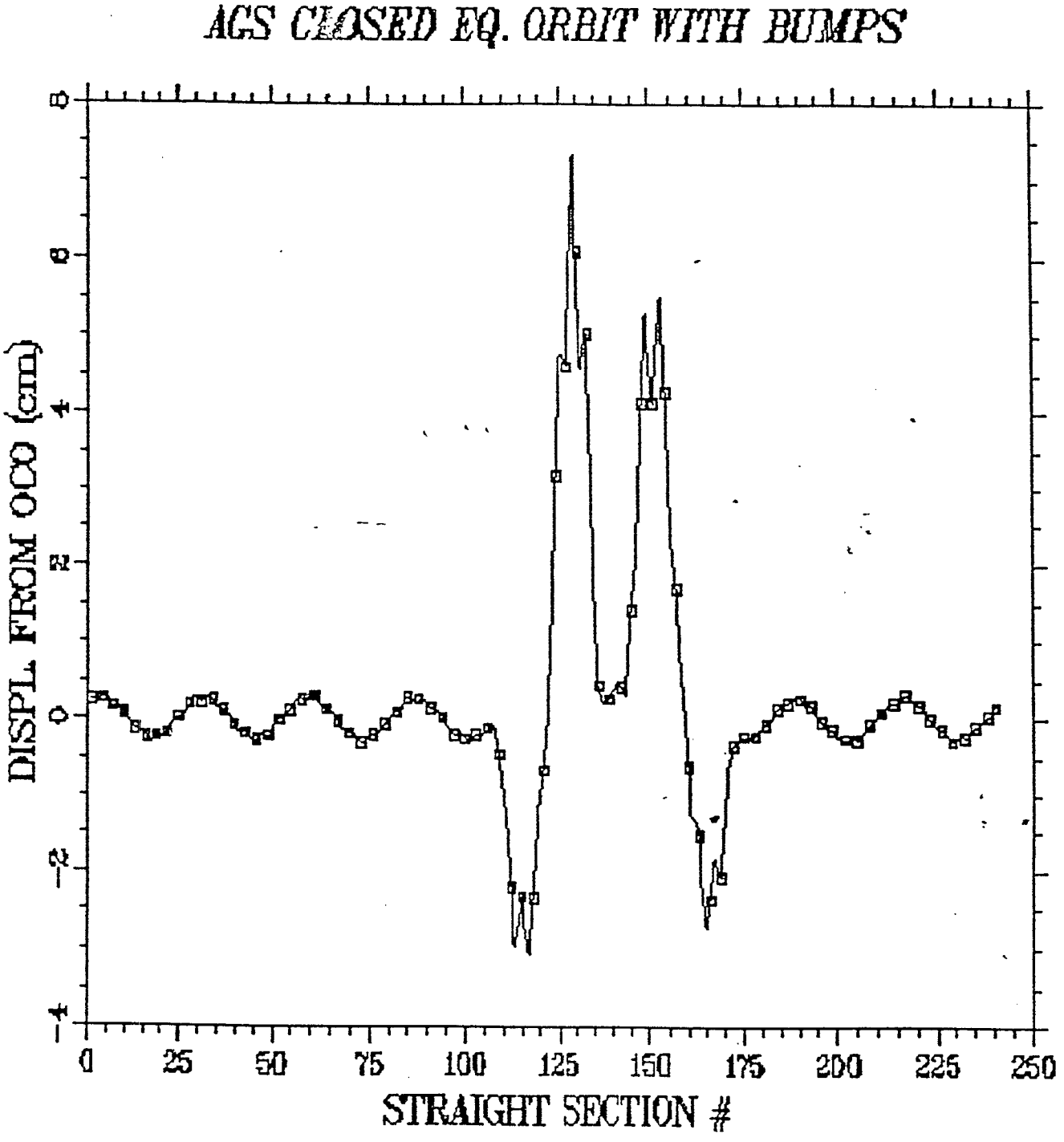

Fig. 7 Displacements of a central closed orbit (in OCO system) in all the straight sections of the AGS. The strength of the bumps is adjusted at G10 and H10 to provide the desired displacement at G10 (SS130) and H10 (SS150) locations, with no regard on the residual oscillations in the region outside the main bumps. The curve is to guide the eye.

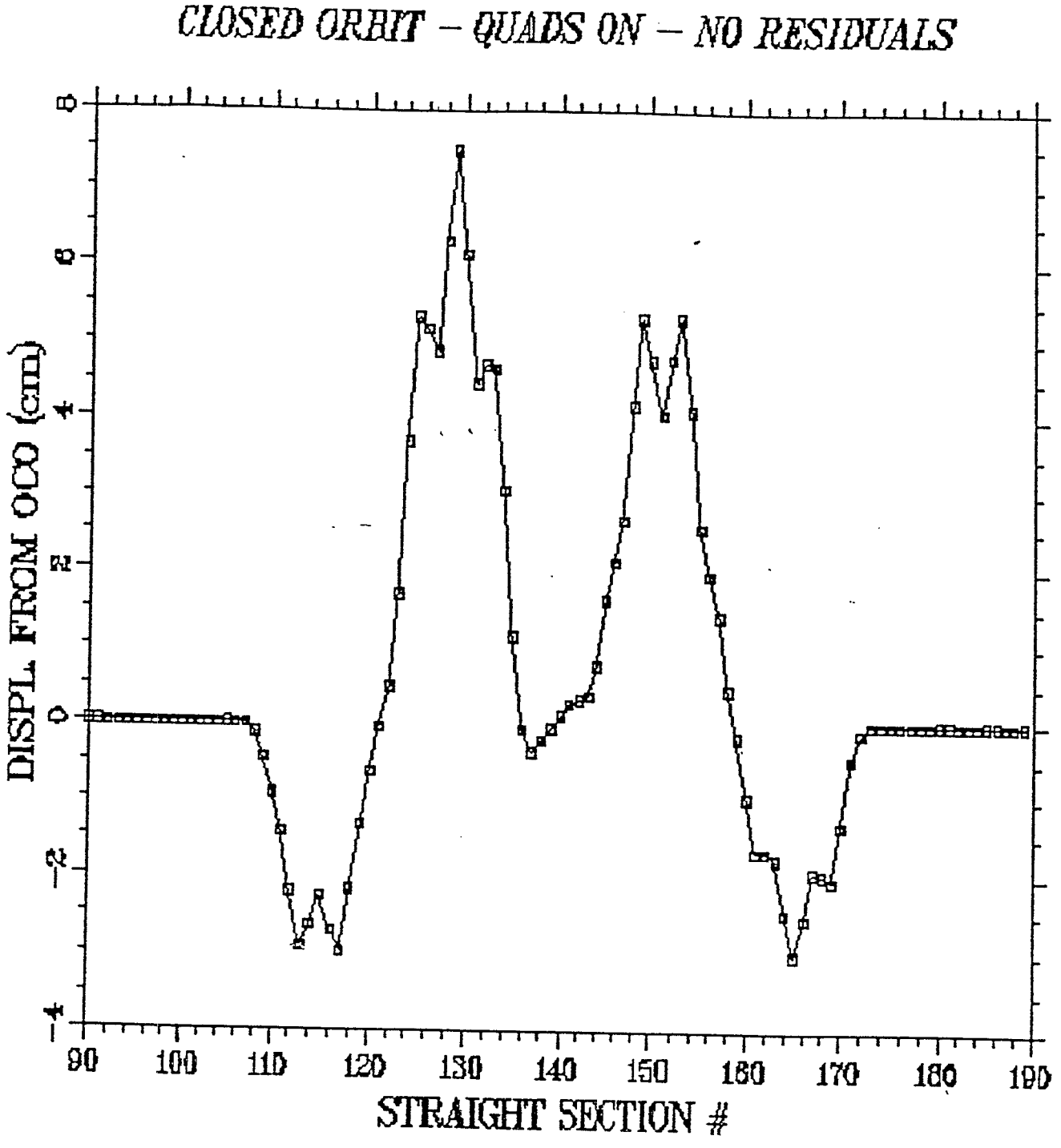

Fig. 8 Displacement of a central closed orbit (in OCO system) in straight sections E10 to J10 of the AGS, with no residual oscillations in the region outside the bumps. The curve is to guide the eye.

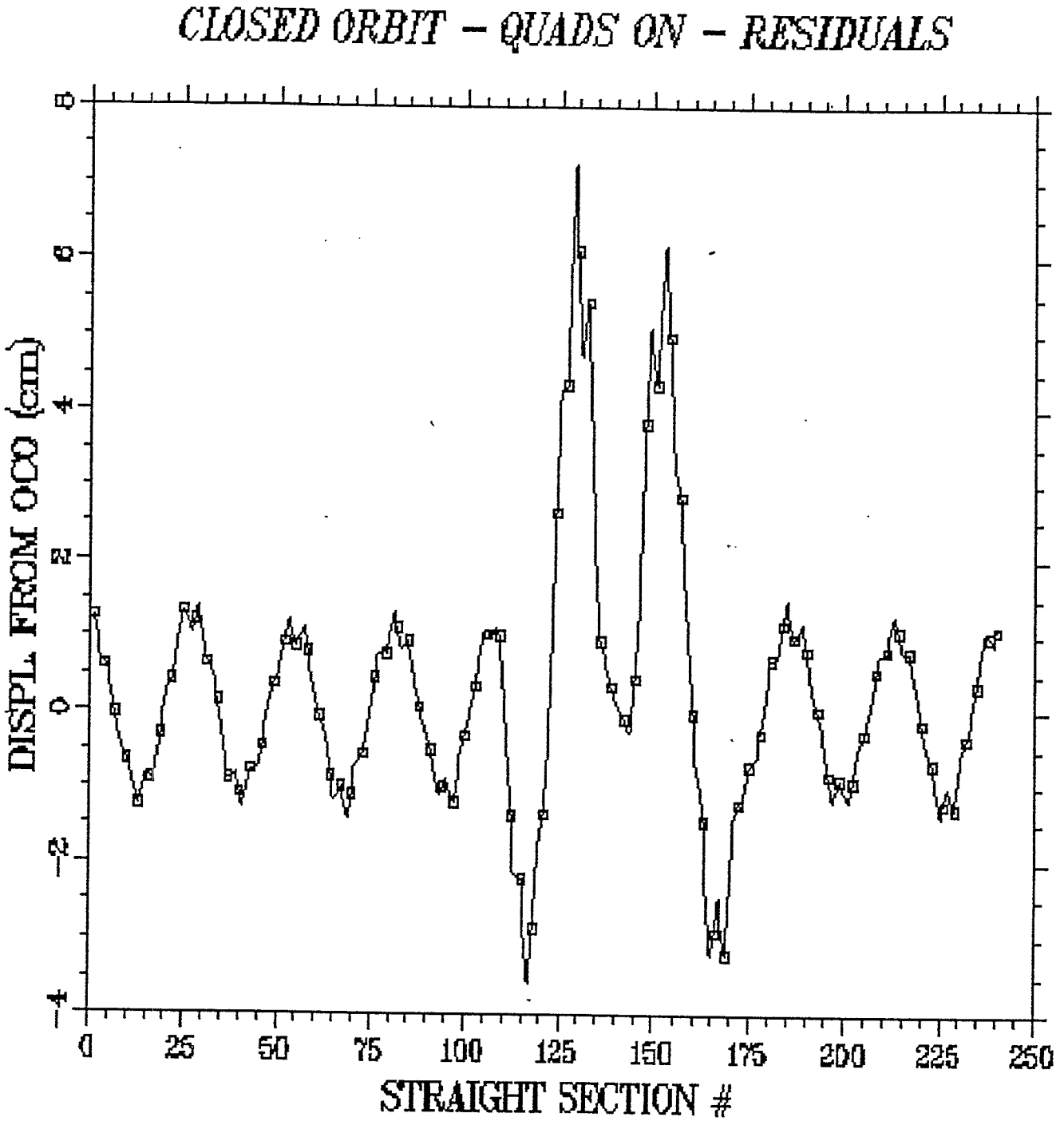

Fig. 9 Displacement of a central closed orbit (in OCO system) in all straight sections of the AGS, no compensation of residuals in the region outside the main bumps. The curve is to guide the eye.

TABLE I
AGS-BEAM PARAMETERS AT H13. (CLOSED ORBIT AT OCO)
(p=29.2305 GeV/c)

	1 BARE MACH. OCO	2 NO/RES	3 W/RES QHV-ON	4 NO/RES QHV-ON	5 W/RES
EXTRACTION AT H13					
β_h (m)		39.33	34.69	34.69	35.09
α_h		-4.07	-3.48	-3.48	-3.54
β_v (m)		7.04	8.14	8.14	7.89
α_v		0.92	1.06	1.06	1.00
η_h (m)		1.44	0.65	0.65	2.04
η_h'		0.1280	0.048	0.048	0.116
G10 Kick (mrad)		-1.651	-1.531	-1.531	-1.519
H10 Kick (mrad)		20.895	21.320	21.320	20.608
VX' -H10 (mrad)		-4.72	-5.14	-5.14	-4.43
DH10 (m)		1.25	0.78	0.78	2.66
D′ H10		-0.04	-0.03	-0.03	-0.13
EQUILIBRIUM ORBIT PARAMETERS					
0.05%	8.69228	8.62588	8.62428	8.80165	8.79700
ν_h = 0.00%	8.67319	8.60632	8.60583	8.78355	8.77993
-0.05%	8.65176	8.58568	8.58796	8.76417	8.76233
0.05%	8.66695	8.69387	8.69471	8.71551	8.71493
ν_v = 0.00%	8.67578	8.70249	8.70282	8.72376	8.7273
-0.05%	8.68683	8.71235	8.71020	8.73296	8.73036
Ξ_h	-40.52	-40.2	-36.3	-37.5	-34.67
Ξ_v	19.88	18.5	15.5	17.5	18.67
Bump 1a		0.980	1.022	0.918	0.904
Bump trim 1		0.000	0.000	0.000	0.000
Bump 1b		1.050	1.022	1.042	0.904
Bump 2a		0.981	0.994	0.871	1.142
Bump trim 2		0.000	0.000	0.000	0.000
Bump 2b		0.950	0.994	1.015	1.142
X'-G10 (mrad)		-5.62	-5.60	-5.92	-5.26
X'-H10 (mrad)		-3.19	-3.08	-3.20	-2.51
η_h (max) (m)	2.17	3.25	3.35	4.05	5.29
η_h (min) (m)	1.46	0.75	0.74	-0.01	-1.38
β_h (max) (m)	22.30	26.49	26.53	28.68	28.17
β_h (min) (m)	10.40	9.62	9.63	8.20	8.46
β_v (max) (m)	22.30	25.54	25.53	26.42	26.80
β_v (min) (m)	10.40	9.02	9.03	7.98	8.35

APPENDIX A1

Determination of the AGS (NEWFEB) Extraction Point H13

The New Fast Extraction Beam (NewFEB) System (Ref 6) is employed to extract the AGS Beam pulses from the AGS to the origin of the AGS-RHIC Beam Transfer Line (Ref. 1), also called the H13 extraction point (see Fig. A1.1). Its location has been determined from calculations which are reported in this Tech-Note. The diagram of Fig. A1.1 shows the layout of the AGS magnets H10, H11, H12, H13, the straight sections H10, H11, H12, H13 and the corresponding Optimum Closed Orbit (OCO). The septum magnet at H10 is considered as a zero length dipole magnet placed at the point X-H10 (Fig. A1.1), it deflects the beam by a given angle. This assumption (of zero length dipole) does not affect the beam trajectory outside the actual septum magnet. The point of the deflection, X-H10, has been set at a distance 7.555 cm from OCO-H10 (7.222 cm from SS-H10). A particle on the central trajectory, deflected by the septum magnet over the proper angle will appear at the extraction point at H-13 with the proper direction to pass through the 4.25° bending point of the U-Line. Between point X-H10 and the extraction point at H13 the particle experiences the fringing fields of the magnets H11, H12, and H13 (as shown in fig. A1.1); thereafter, it continues through a field-free region. The extraction point H13 can be defined as the intersection of two lines: the normal at the center of straight section H13 and the central particle trajectory that passes through the 4.25° bending point. The calculation of the central orbit inside the AGS and in the extraction region is done by the computer code BEAM, modified to accept measured magnetic fields. (See Appendix A2)

Table A1.I contains the coordinates (both in the OCO system and the AGS system) of the most important points during the beam extraction. These points are marked with filled circles on fig. A1.1. Fig A1.2, A1.3 and A1.4 (top) show a cross section normal to the axis of the H11, H12, and H13 AGS magnets and the location (indicated by arrows) of the central trajectory at the entrance and exit of the magnets. Fig A1.2, A1.3, A1.4 (bottom) show the magnetic field that a particle experiences in the magnets H11, H12 and H13 during the extraction process. In Fig. A1.2, A1.3 and A1.4 all horizontal distances are measured with respect to the magnetic axis of each magnet. AGS magnet H13 is a "closed" C-type magnet and its field has been measured from -7.4" to 8.6" (Fig. A1.4). Therefore, the extracted central trajectory lies well beyond the region of the measured field for the H13 magnet (Fig.

A1.4). In order to provide BEAM with magnetic field data for the associated section of the particle trajectory, we have taken the following three steps:

1. We performed a two dimensional magnetic field calculation of a C-type AGS magnet using the computer code OPERA (Ref. 8), the excitation current was chosen to obtain the best match ($<10^{-3}$) between the calculated and the measured fields inside the aperture of the magnet.

2. Then we fitted a (9th order) polynomial to the calculated fields in the region from 8" to 17".

3. The coefficients of that polynomial were entered as data into the computer code BEAM so that the code can calculate the magnetic fields required for trajectory calculations when the particle is in the region where there are no experimentally measured magnetic fields.

ID NAME	OCO-SYSTEM		AGS-SYSTEM	
	Distance (cm)	Direction (mrad)	East (inches)	North (inches)
OCO-H10	0.0	0.0	11320.85644	14527.68655
SS-H10	0.3332	0.0	11320.97005	14527.85315
X-H10	7.556	16.174	11327.40014	14528.18655
OCO-H13	0.0	0.0		
SS-H13	0.4854	0.0	11114.63997	14858.65784
X-H13	45.086	69.5422	11129.14664	14868.55193
B_4.25			10893.95856	15270.84365

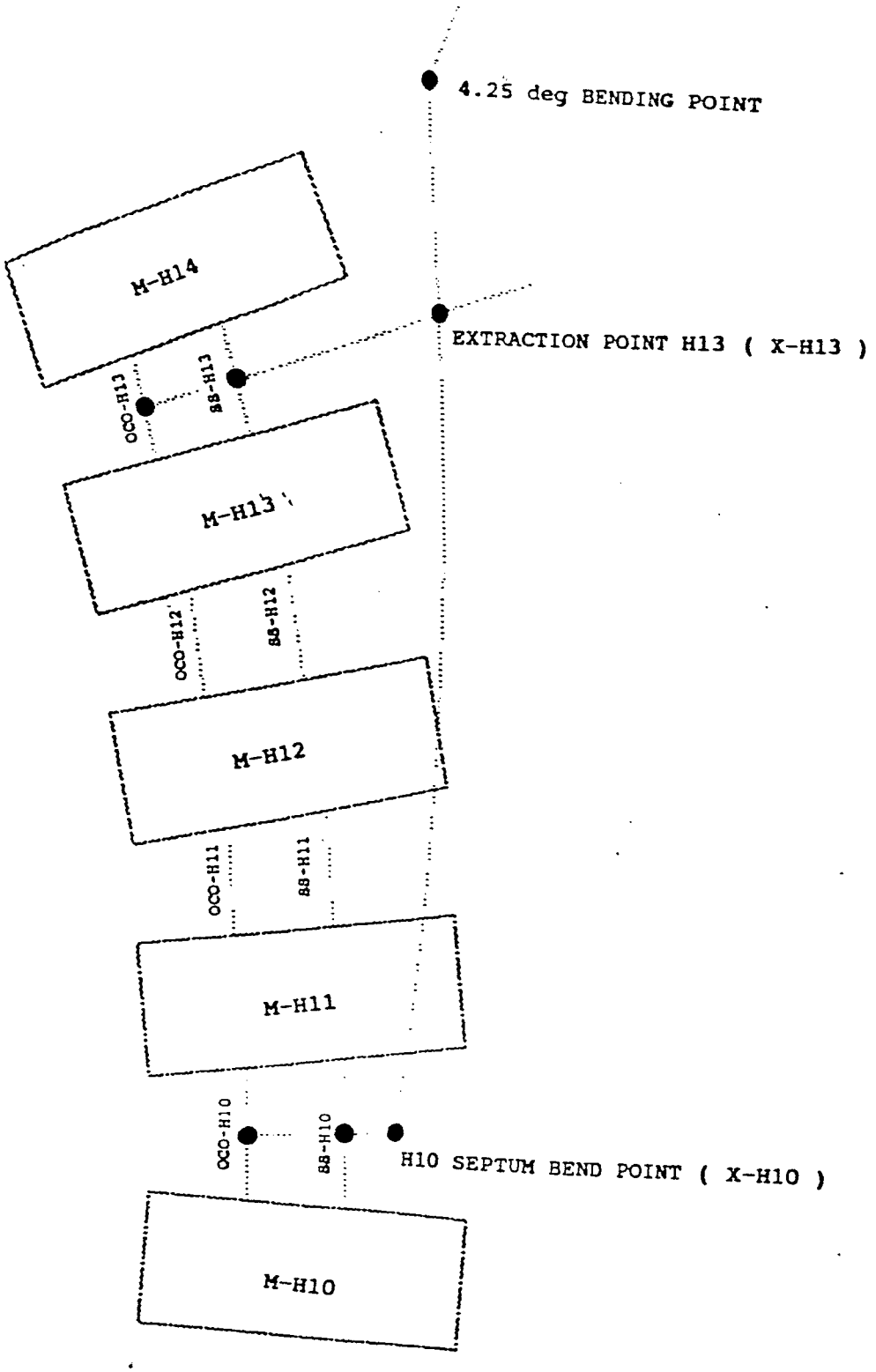

Fig. A1.1 Diagram of the extraction region near the extraction point at H13. The abbreviations (M), (SS-), and (OCO-) specify a Magnet, Straight Section, and Optimum Closed Orbit respectively. The most important points which are discussed in the text, show as large full circles. Tabulation of the coordinates of the points which are marked as full circles appear in Table A1.I.

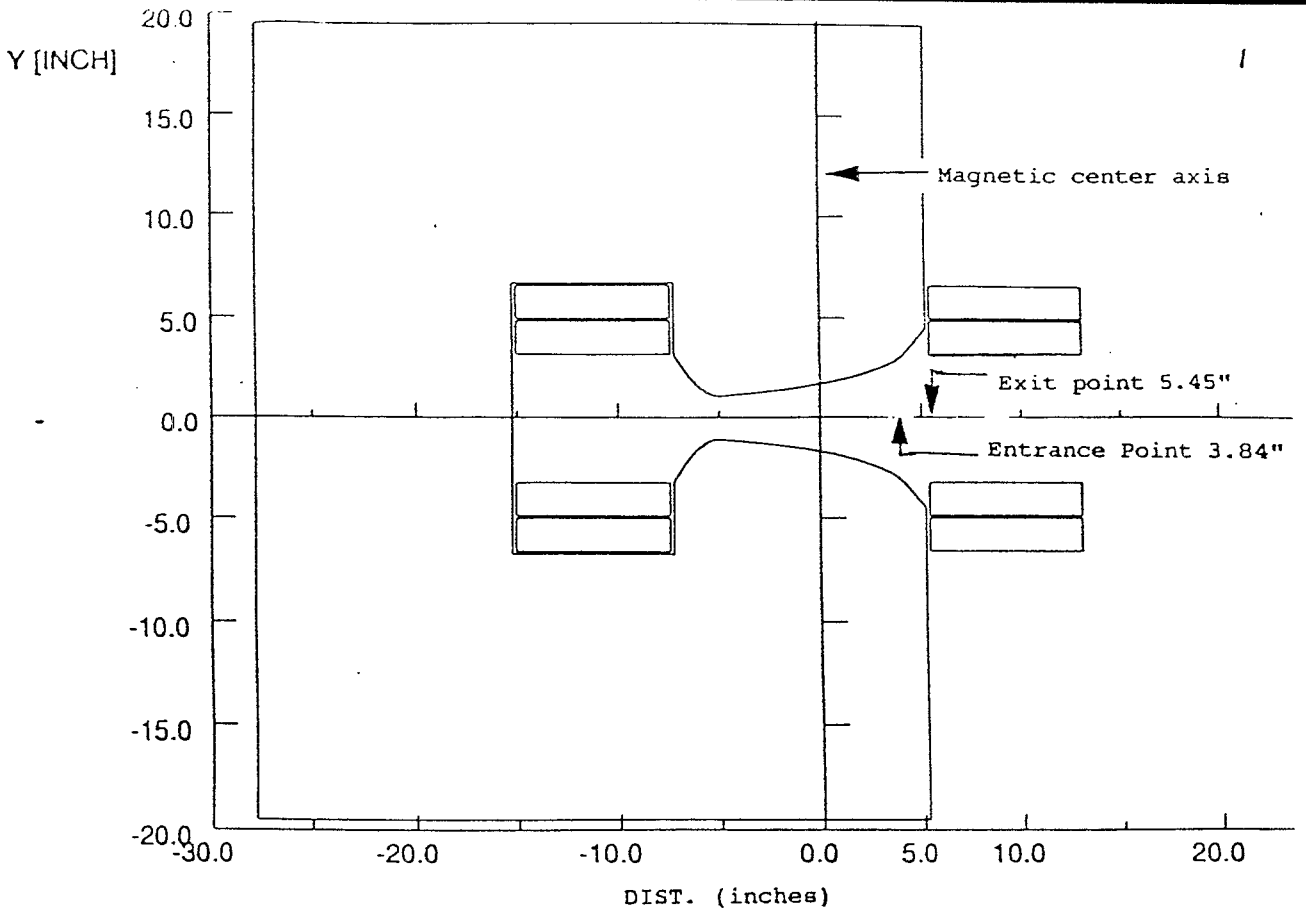

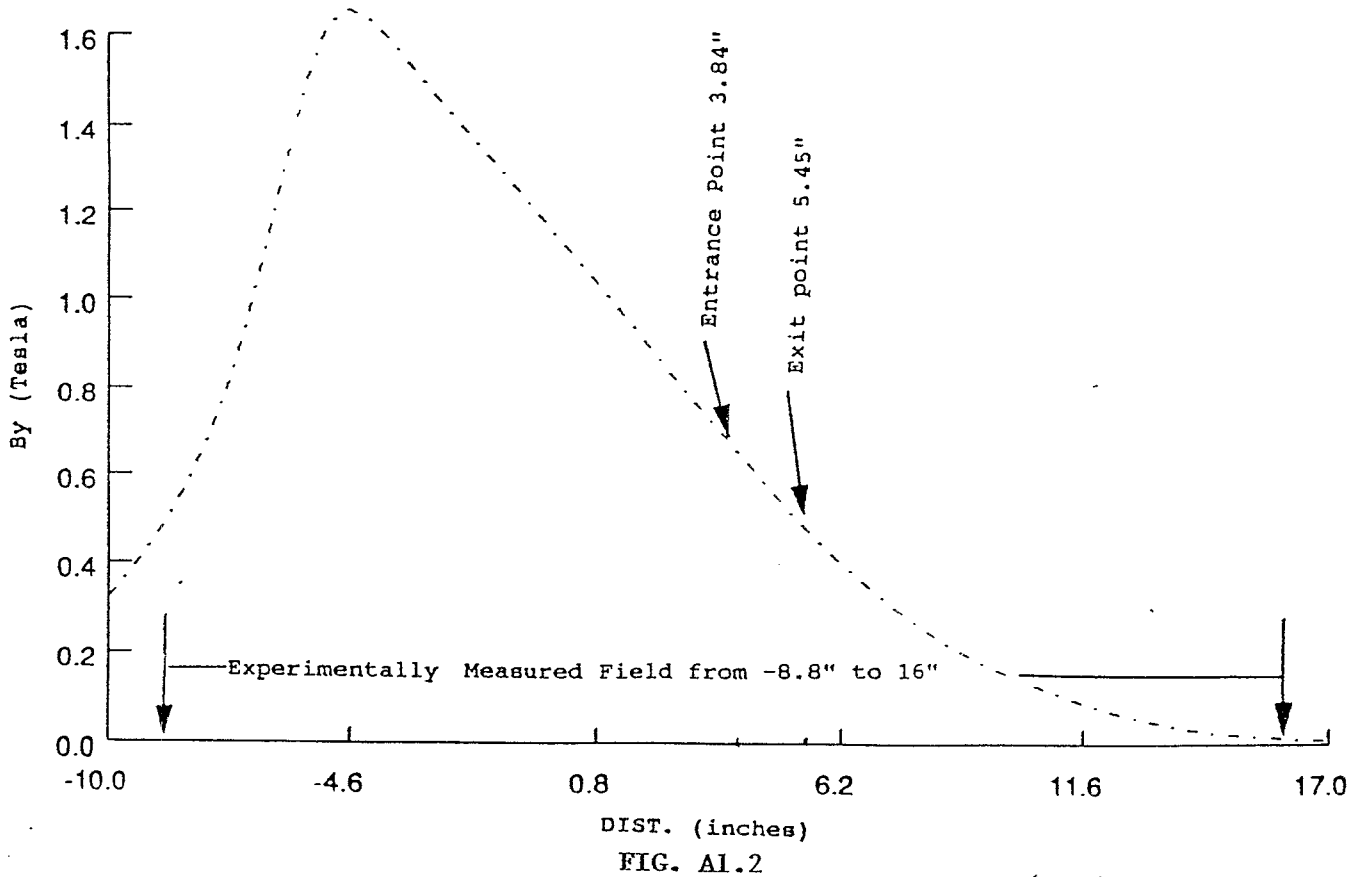

FIG. A1.2

Fig. A1.2, A1.3, A1.4 Cross section of the AGS magnets H11 to H13 (top) and their corresponding magnetic field at the median plane (bottom). The points of entrance and exit of the extracted beam axis orbit are indicated by arrows.

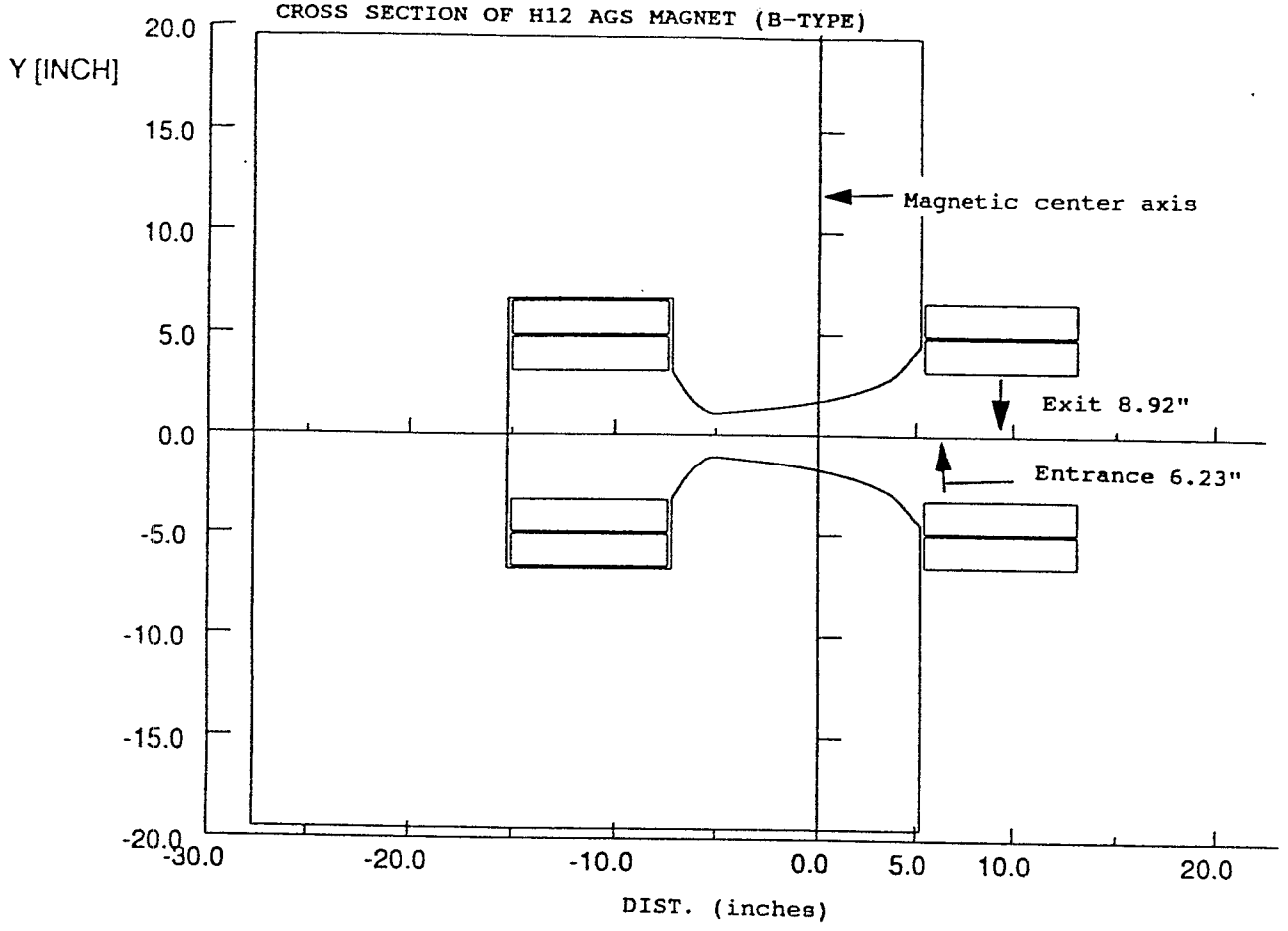
CROSS SECTION OF H12 AGS MAGNET (B-TYPE)
Y [INCH]
20.0
15.0
10.0
5.0
0.0
-5.0
-10.0
-15.0
-20.0
-30.0
-20.0
-10.0
0.0
5.0
10.0
20.0
DIST. (inches)
Magnetic center axis
Exit 8.92"
Entrance 6.23"

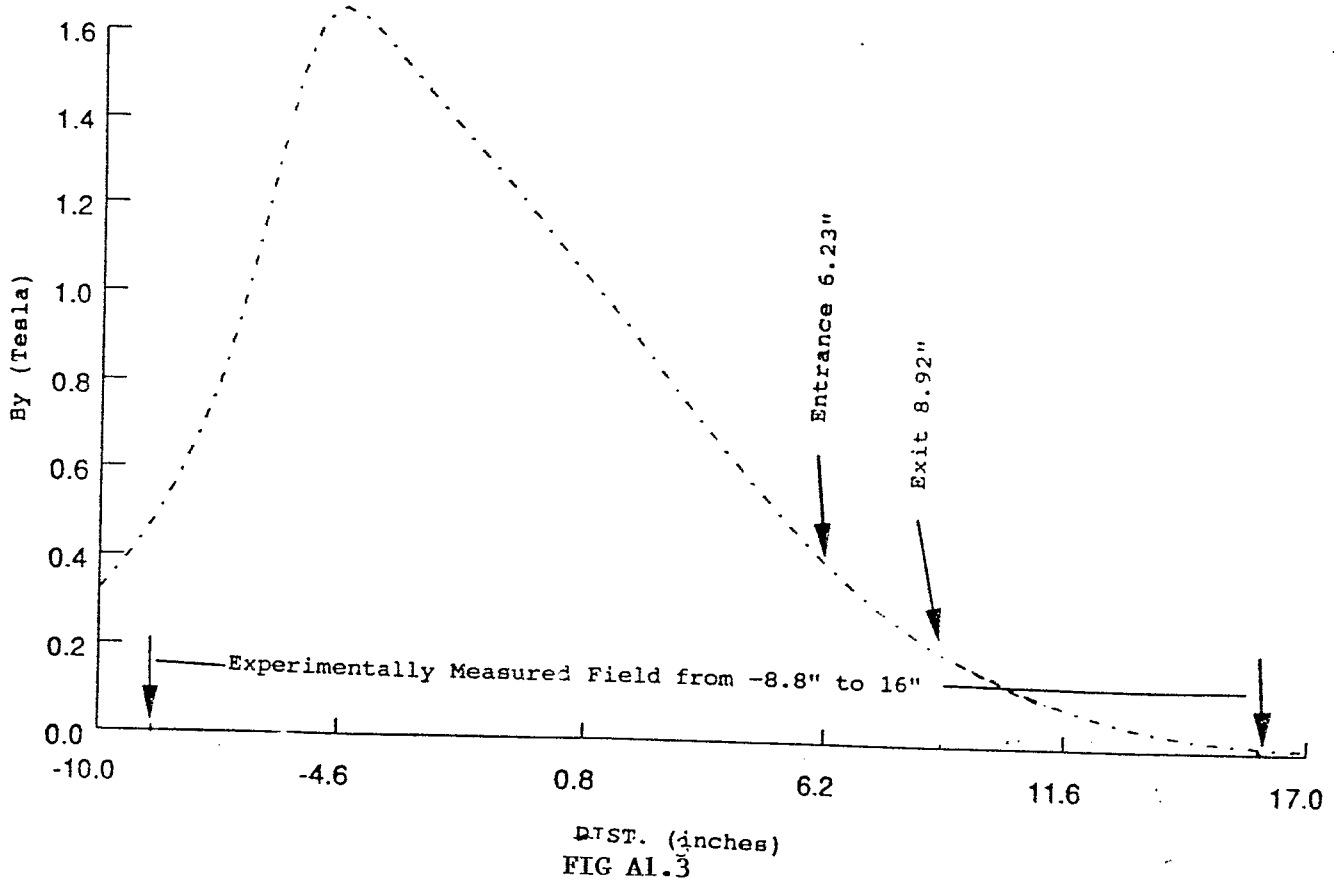
By (Tesla)
1.6
1.4
1.2
1.0
0.8
0.6
0.4
0.2
0.0
-10.0
-4.6
0.8
6.2
11.6
17.0
DIST. (inches)
Entrance 6.23"
Exit 8.92"
Experimentally Measured Field from -8.8" to 16"

FIG A1.3

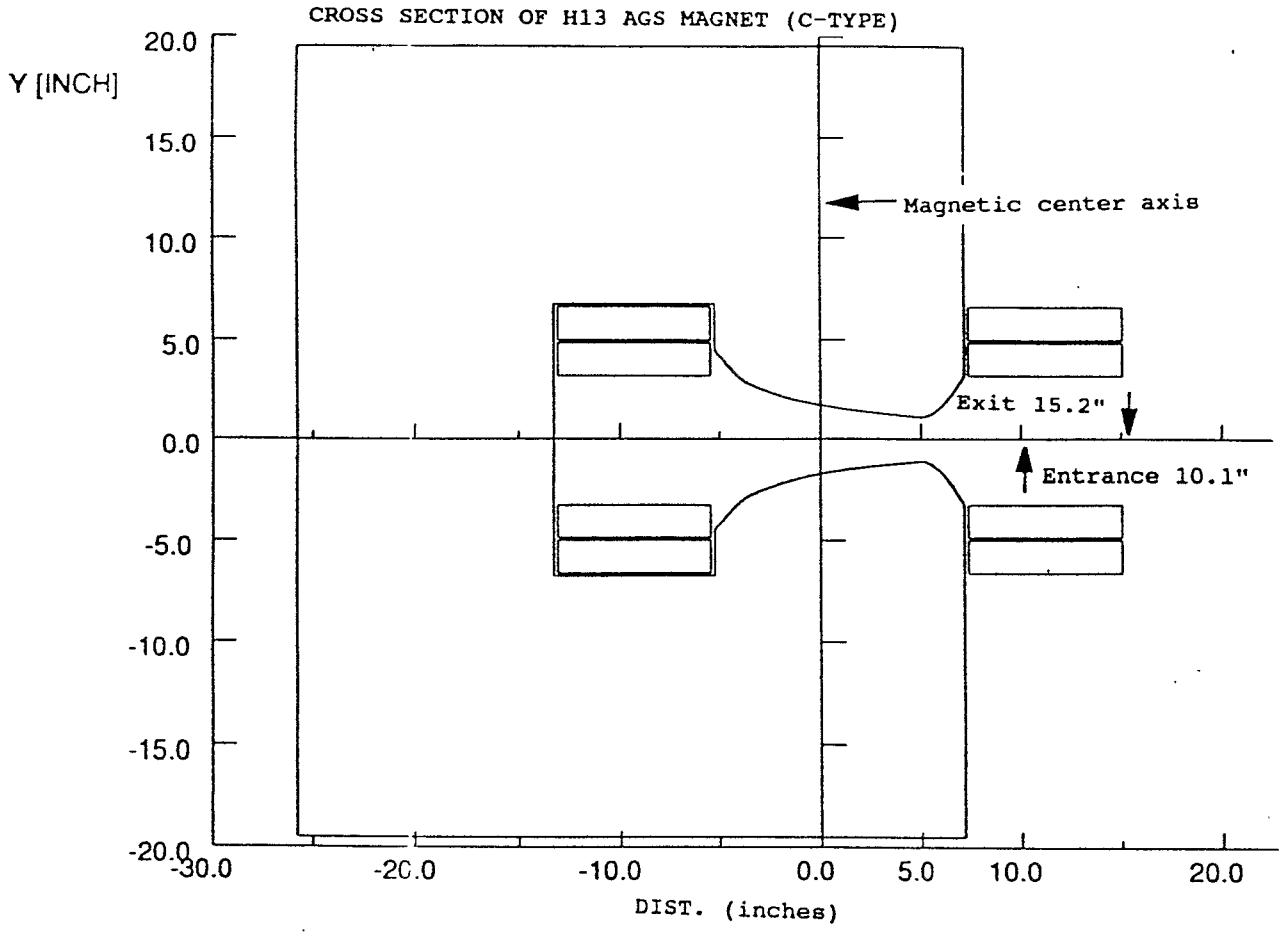
CROSS SECTION OF H13 AGS MAGNET (C-TYPE)
Y [INCH]
20.0
15.0
10.0
5.0
0.0
-5.0
-10.0
-15.0
-20.0
Magnetic center axis
Exit 15.2"
Entrance 10.1"
-30.0
-20.0
-10.0
0.0
5.0
10.0
20.0
DIST. (inches)

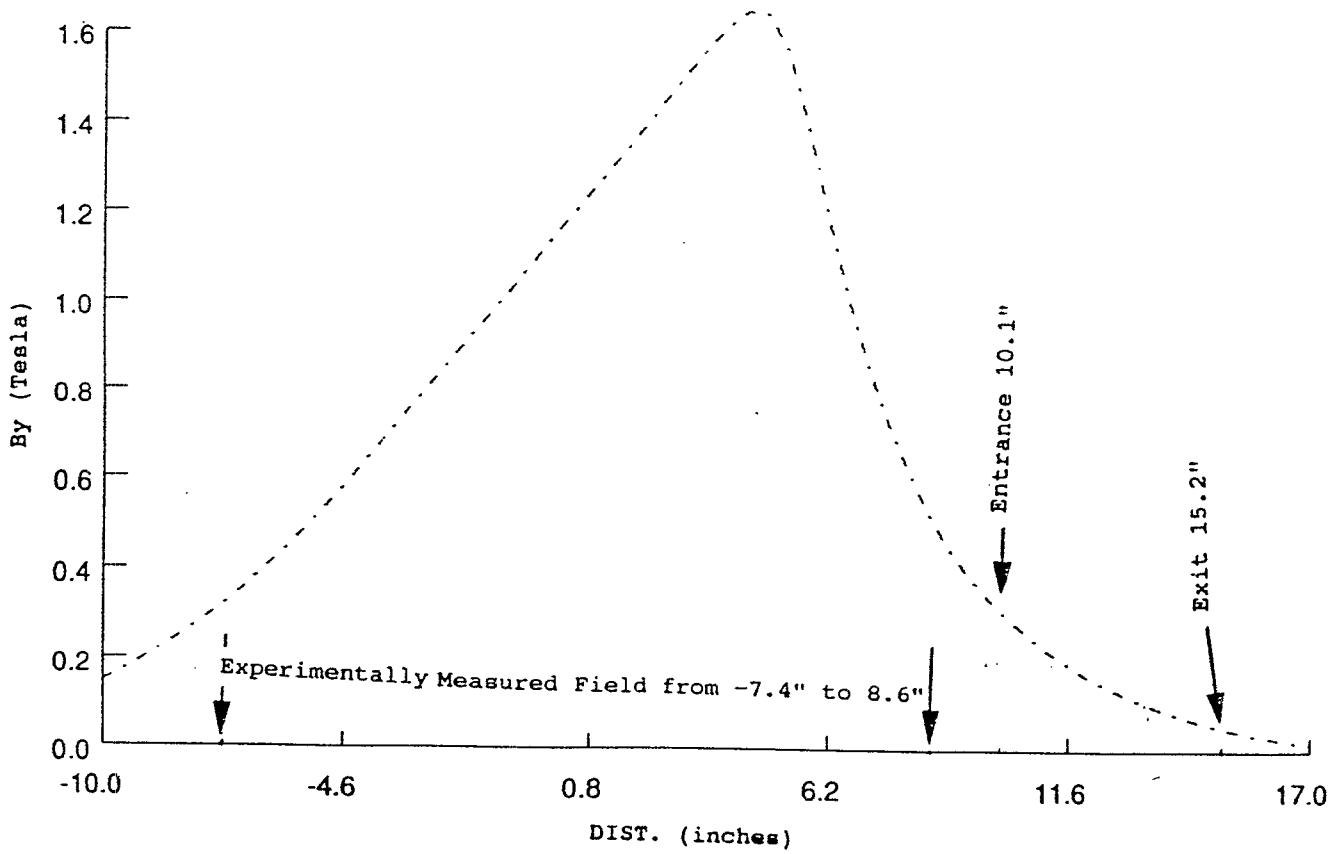
By (Tesla)
1.6
1.4
1.2
1.0
0.8
0.6
0.4
0.2
0.0
Entrance 10.1"
Exit 15.2"
Experimentally Measured Field from -7.4" to 8.6"
-10.0
-4.6
0.8
6.2
11.6
17.0
DIST. (inches)

FIG A1.4

APPENDIX A2

Magnetic Field Maps and their Implementation in the Beam Code

Reference 7 provides a description of the 240 AGS magnets, their coordinates in the AGS ring, most of the nomenclature developed for the survey of the magnets, as well as references concerning the AGS. There are three types of combined function magnets, identified as type A, B and C. Fig. A2.1 shows the cross sections of these magnets. Type A and B magnets have identical cross sections but different lengths of 90 and 75 inches respectively. Magnet Type C has a length of 90 inches. These combined function magnets act as, and may be regarded as sections of, focusing or defocusing quadrupoles, depending on their orientation with respect to the beam axis, see Fig. A2.1. Both a magnet of type A and a magnet of type C were magnetically mapped (Ref.5) over a rectangular area (Fig. A2.2) in the median plane of each magnet. Since magnet types A and B have identical cross sections, magnet type B was not mapped, it is assumed that its field in the direction transverse to the long axis of the magnet and its edge fields are identical to the field of the magnet type A. The thick solid lines in Fig. A2.2 is the projection on the median plane of the outline of the iron core of the magnets. Magnet type A was mapped over two separate rectangular grids G1 (ABCD) and G2 (EFGH) (Fig. A2.2 top). Grid G1 extends from -17 inches to +45 inches in the z-direction and from -8.8 inches to 7.2 inches in the x-direction. Grid G2 extends over the same distance as grid G1 in the y-direction, and from 0 inches to 16 inches in the x-direction. The origin is taken to be the intersection of three planes:

a) The median plane;

b) The plane which contains the entrance edge of the magnet and is normal to the median plane;

c) The plane passing through the socket line (Ref. 7) and normal to the median plane.

Grid G1 provided the magnetic field data required to calculate the particle trajectory unless the particle was located beyond 7.2 inches in the x-direction; then the data from grid G2 was used. Magnet type C was mapped over a single rectangular grid G1(ABCD) which extends from -17 inches to 45 inches in the z-direction and from -7.4 inches to 8.6 inches in the x-direction (Fig. A2.2 bottom). The origin is defined similarly as for magnet type B above. The grid step size is 0.1 inches in the

x-direction, amounting to a total of 161 grid points. The grid step size in the y-direction is 1 inch except in the region -5.0 to 5.0 inches where it is 0.25 inches; this generates 93 grid points. In order to use these field maps the computer code BEAM, which performs the particle tracking by Runga Kata integration, one has to provide a procedure that smooths the experimental magnetic field data at the grid points, and a procedure for calculating the magnetic field at any point in the median plane. This was done as follows. First we selected specific grid points (I,J) based on the algorithm I=3*(i-1)+4 for the x-direction and J=2*(j-1)+3 for the y-direction, with i,j being integers. These points (I,J) are shown as filled circles in Fig. A2.3, these points as well as those represented by the open circles, represent points where the magnetic field was measured. Each pair (I,J) represents a grid point which is the center of a rectangular grid (one of these rectangular grids is labeled EFGH in Fig. A2.3) which contains 7 grid points in the x-direction and 5 grid points in the y-direction (outlined rectangles ABCD and EFGH in Fig. A2.3). It is obvious that a rectangle centered on the grid point (I,J), will overlap with the rectangles centered on grid points (I, J ± 1) (I ± 1, J) (I ± 1, J ± 1). Each of these rectangular grids contains 7x5 grid points where the magnetic field was measured, we fit the function:

$$B_z(x,y)=\sum_{k=0}^{5}\sum_{m=0}^{3} C_{IJkm}\, x^k y^m$$

to these experimental points. The coordinates (x,y) in the formula above are local coordinates with respect to the center (I,J) of the rectangular grid defined above, B_z represents the magnetic field component normal to the medium plane at point (x,y). The coefficients C_{IJkm} obtained from the fits of B_z to each set of 7x5 experimentally measured points, are calculated and stored in a four dimensional array. Then BEAM calculates the magnetic field at any given point in the median plane using the following procedure: for a given (X,Y) location in the median plane the routine finds the 7x5 rectangle whose center is nearest to the particle location. Then it calculates the coordinates (x,y) of that location relative to the center of that rectangle. Finally the magnetic field at the point (X,Y) is calculated using the formula:

$$B_z = \sum_{k=0}^{5} \sum_{m=0}^{3} C_{IJkm}\, x^k y^m$$

The field derivatives dB_z/dx and dB_z/dy are also calculated after the formula above is differentiated. As part of the field map data manipulation, we computed also the effective magnetic dipole length and effective magnetic quadrupole length. These were calculated using the formula;

$$Leff = (\ell_2 - \ell_1) \frac{\int_{o_1}^{\ell_2} f d\ell}{\int_{\ell_1}^{\ell_2} f d\ell}$$

where f stands for the magnetic field B_z or its Gradient dB_z/dx (the direction of x is the normal to the magnet axis) and $\ell_1 = 52$ inches, $\ell_2 = 62$ inches, are lengths shown in Fig. A2.4. Fig. A2.5 shows the values of the effective dipole and quadrupole magnetic lengths as a function of x for an AGS type A or B magnet (top) and type C (bottom). To summarize, this appendix describes the method we used to reduce the experimentally measured magnetic field data to a set of coefficients C_{IJkm}. This reduction was done by a computer program and the calculated coefficients were stored into a computer file as four dimensional array. The BEAM code was modified to read these coefficients and to calculate, as described above, the normal component of the magnetic field and its gradient at any point on the median plane.

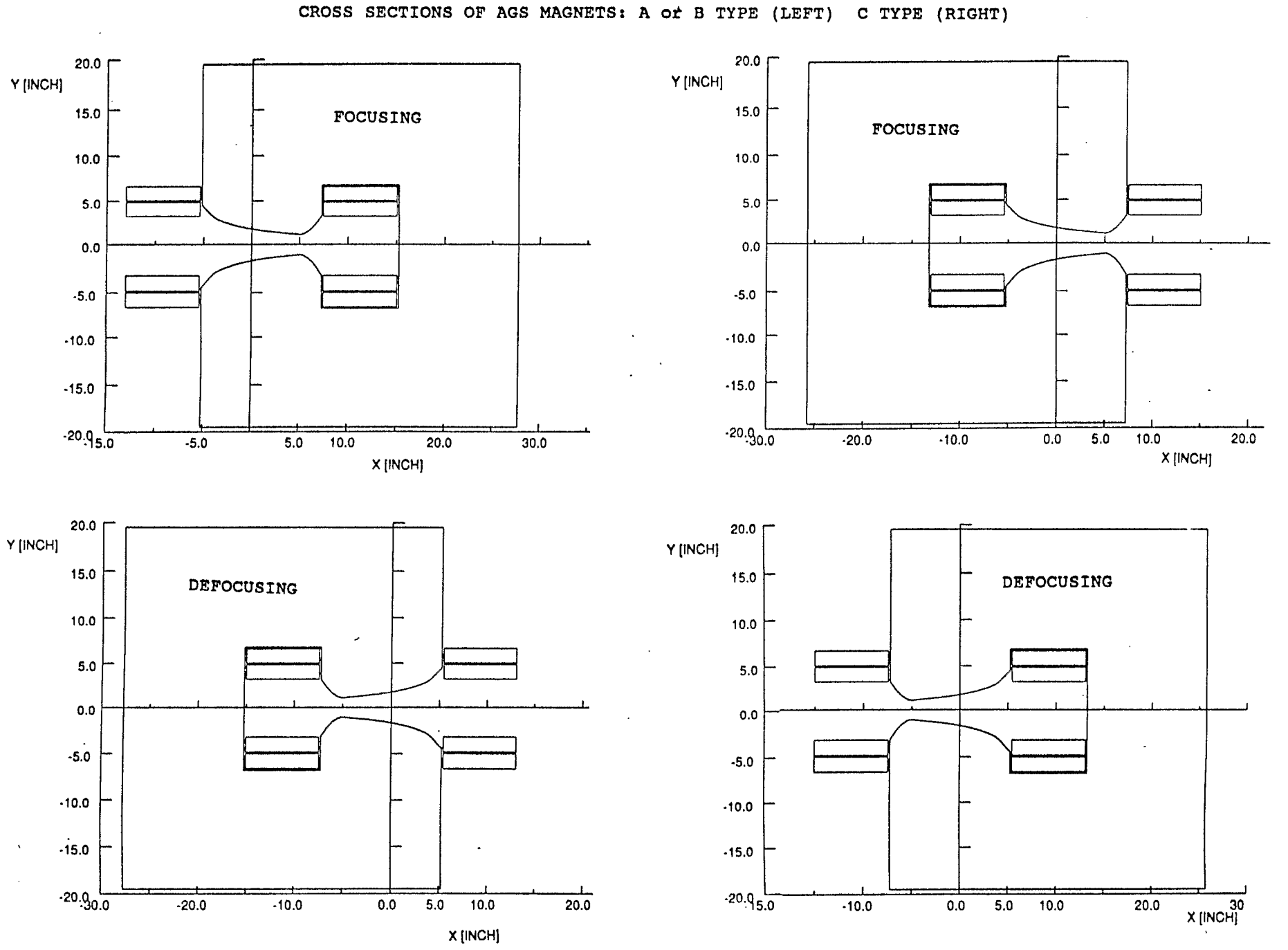

Fig. A2.1 Cross section of the AGS combined function magnets; A or B type (left) and C type (right). The orientation of a magnet relative to the center of the AGS ring determines whether it is focusing (top) or defocusing (bottom).

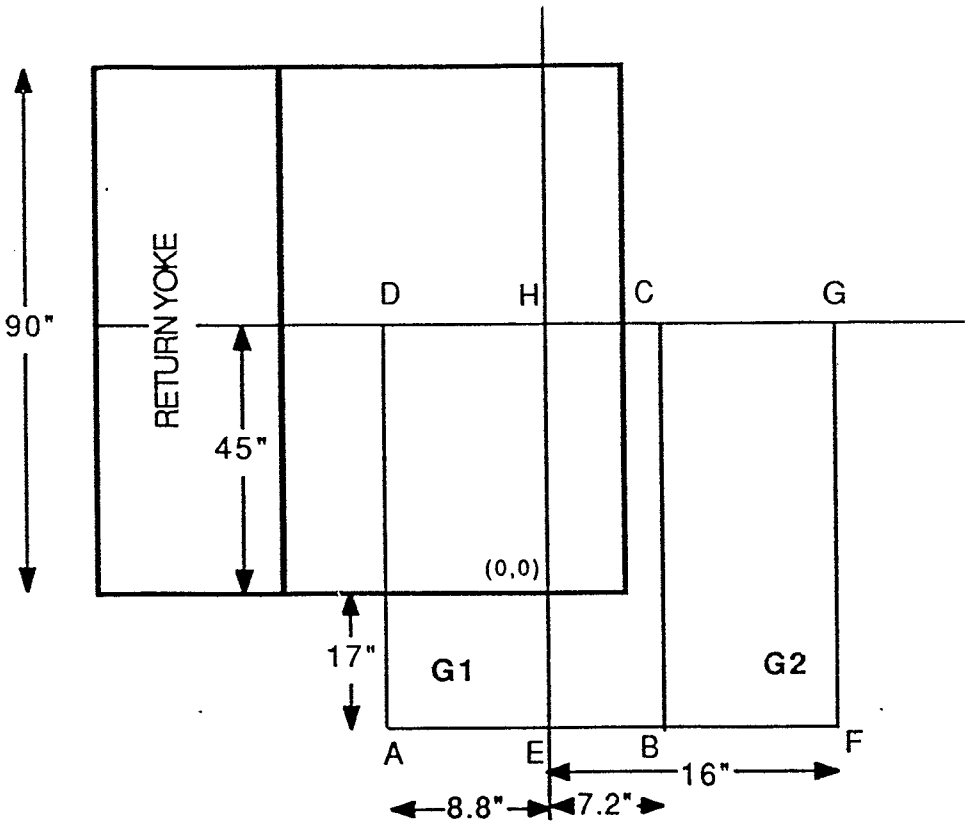

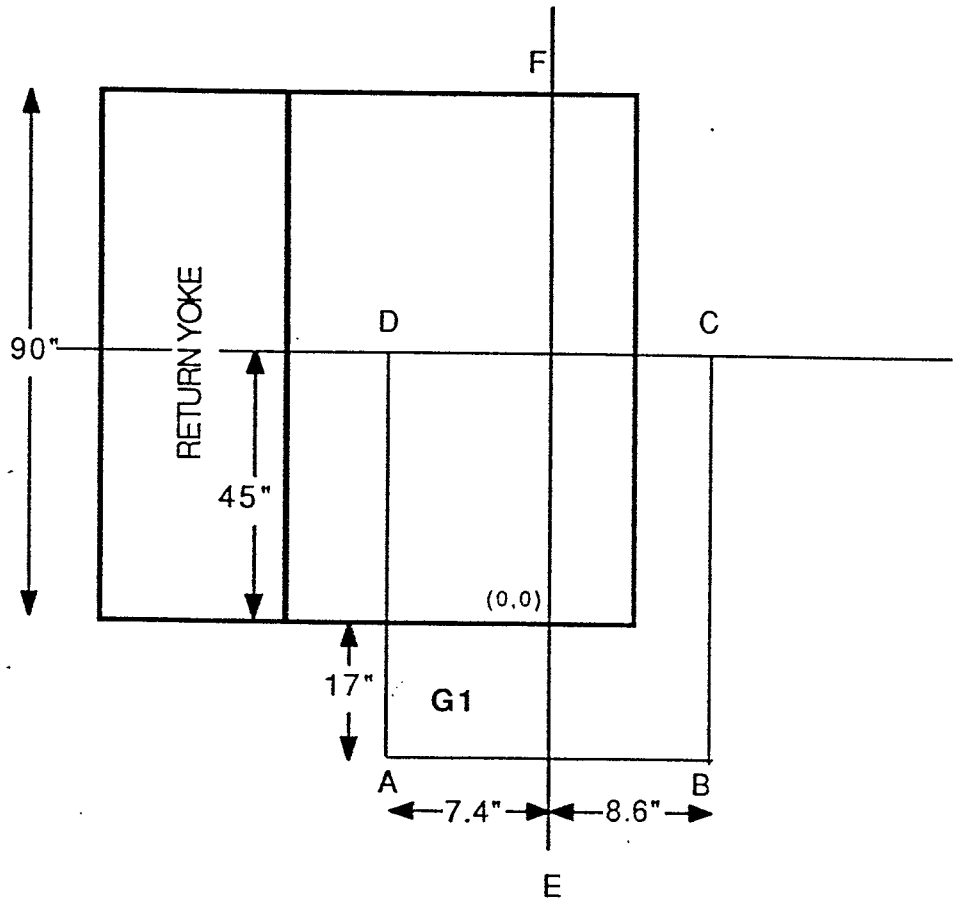

Fig. A2.2 Top: Diagram of the rectangular areas (ABCD) and (EFGH) over which the magnetic field mapping of AGS magnet type A was performed. The heavy line is the outline of the iron core of the magnet. Bottom: Same as in the top diagram but for AGS magnet type C.

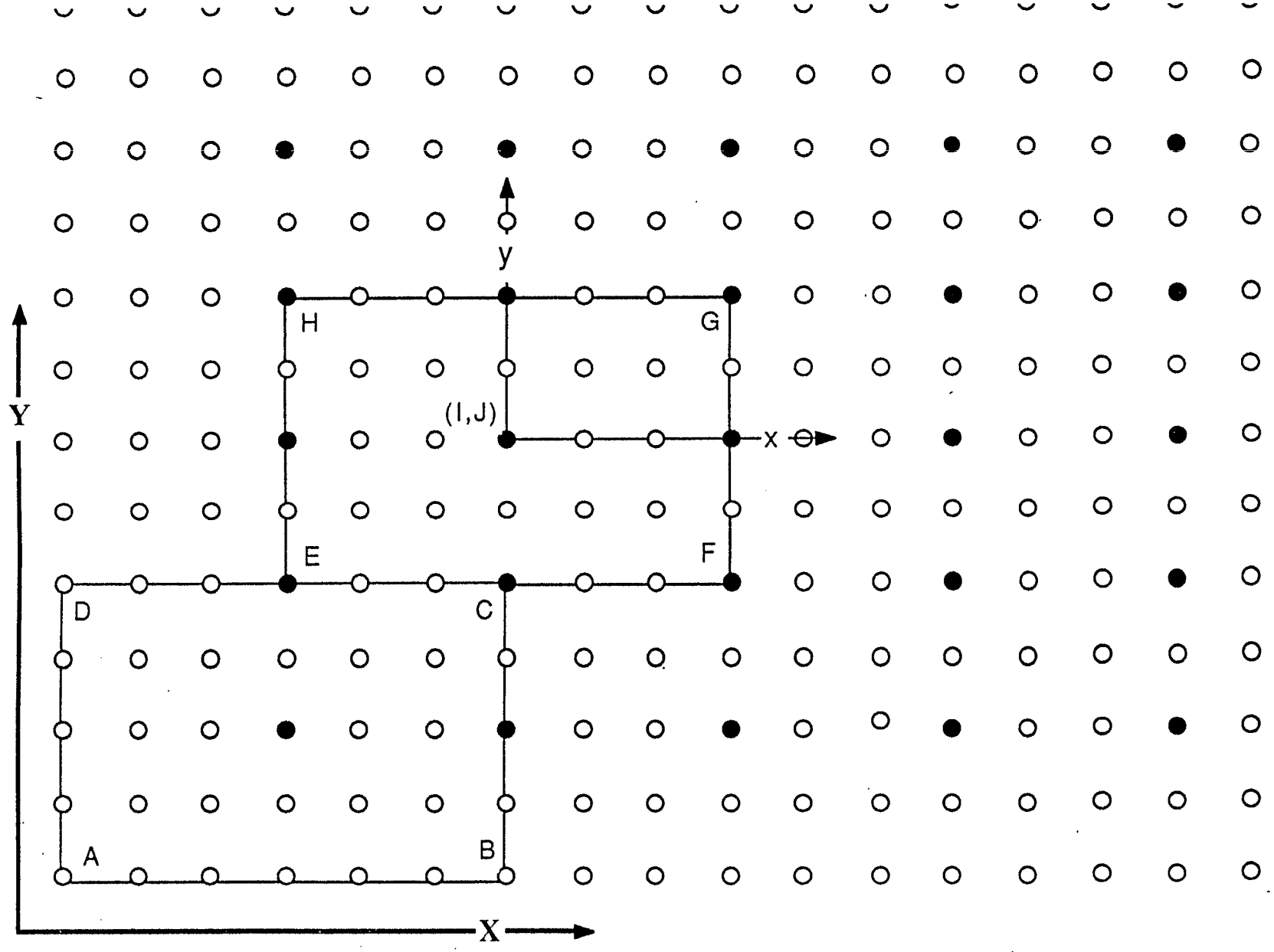

ig. A2.3 Diagram of a section of the rectangular region in which magnetic field mapping was performed. The open and filled circles represent oints of measurement.

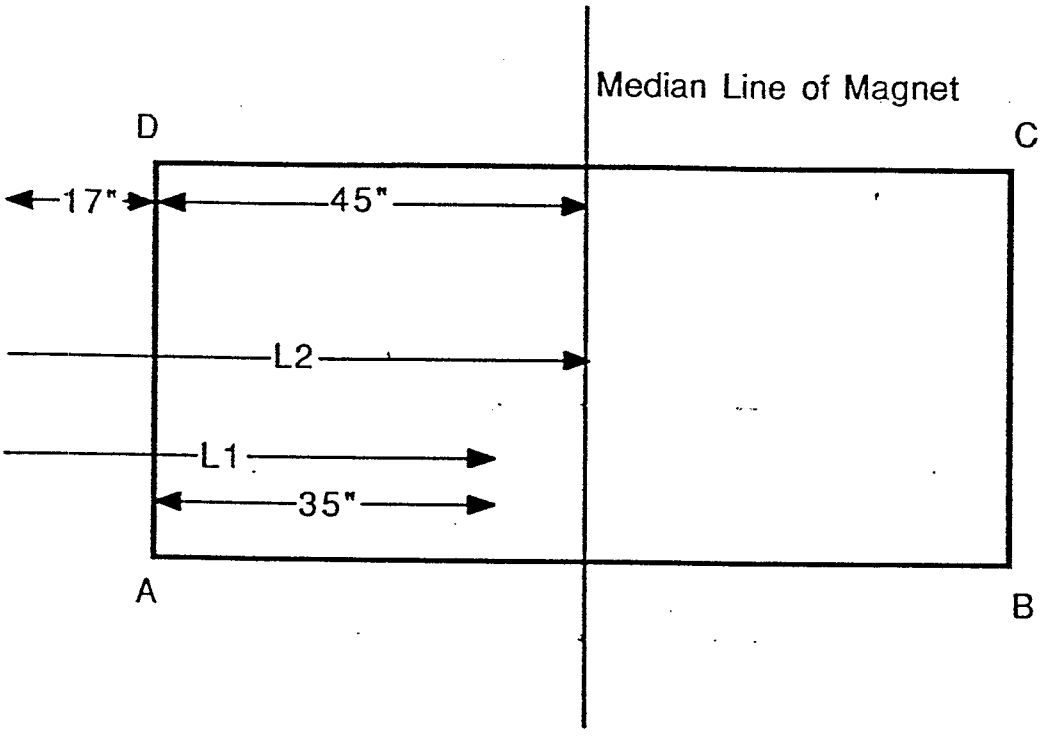

Fig. A2.4

Diagram of the median plane of a magnet.

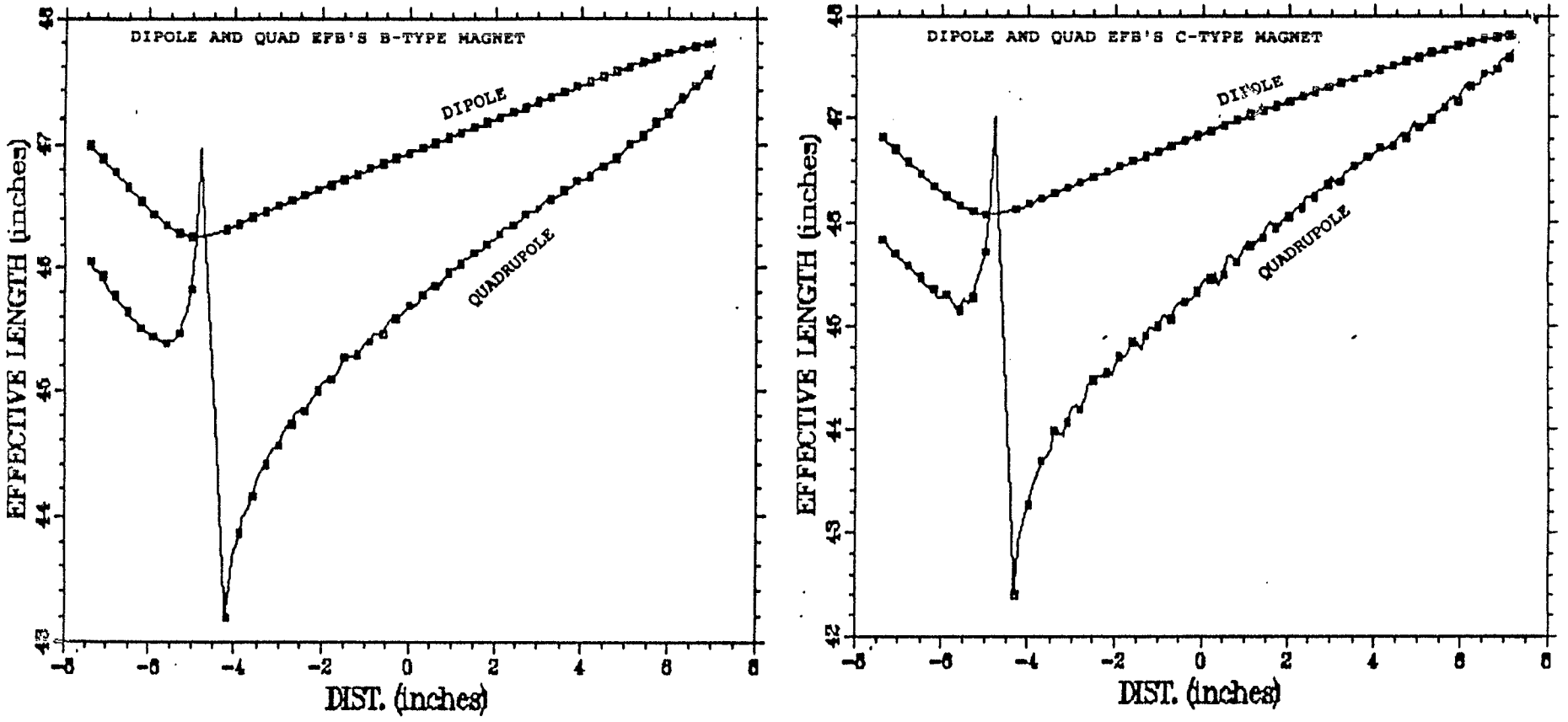

ig. A2.5 The effective magnetic lengths for the dipole and quadrupole components for the B type magnet (top) and C type magnet (bottom) s a function of the distance normal to the long axis of the magnet. There is an apparent discontinuity of the quadrupole effective length at the =-4.50inches. This is due to the fact that the gradient dBz/dx at x=-4.50inches is equal to zero.

APPENDIX A3

Modification to Beam

In this appendix we discuss the modifications made in the computer code BEAM. The source of the code was transferred, from a PDP-10 computer at AGS to the BNL VAX computer cluster at CCD in 1993. The following modifications were made to the BEAM code after it was transferred into the VAX cluster:

a) The QUAD and SEXT subroutines of the BEAM code were modified to align the longitudinal axis of the AGS quadrupole and sextupole elements with the OCO (Optimum Closed Orbit), instead of the SS-line (see definition of Straight Section line in ref. 7). This was necessary since the axes of the AGS Quads and Sextupoles are now aligned relative to the OCO.

b) New extraction bump coils and two trim bump coils were modeled in the BEAM code. The location of the new extraction bump coils is described in ref. 6, a summary of the locations and strengths of these bump coils as well as of the trim bump coils is presented in Table A3.I. The function of the trim bumps (ref. 10) is to minimize any residual oscillations of the AGS central orbit in the region outside the bumps.

c) The strength of each bump coil is entered into the code as the value of $\Delta\theta/\theta$, where θ is the nominal bending angle of the magnet within the coil, and $\Delta\theta$ is the change of that angle due to the excitation of that coil. A negative $\Delta\theta$ corresponds to an increase of the deflection angle, thus to an increase of the magnet strength. Table A3.I shows the list of magnets supplied with bump coils (column 1,2). Column 5 shows the number of backleg windings which in effect constitute the bump coil. Column 6 shows the maximum strength of each bump coil in mrad and column 7 its the maximum strength in terms of $\Delta\theta/\theta$. The trim bump coils are powered by independent power supplies and the main bump coils are powered by four

independent power supplies labeled 1a, 1b, 2a, 2b in Table I.

d) In the computer code BEAM we have chosen to change the momentum of the particle when it passes through a magnet with a bump coil, instead of changing the magnet strength. Thus a particle with momentum p_0 is given a momentum $p=p_0/(1-\Delta\theta/\theta_0)$ during its passage through a magnet with a bump coil strength $\Delta\theta/\theta_0$.

e) The entrance angle of the magnets, M03, M13, and the exit angle of M08, M18 magnets of each superperiod has been changed in the BEAM code from the value of 16.66 mrad to 16.12 mrad. Likewise, the exit angle of the magnets M03 and M13 and the entrance angle of the M09, M19 magnets of each superperiod has been changed from the value of 9.07 mrad to 9.61 mrad. These new values represent the ideal values to which the AGS magnets should be aligned if the central orbit is to coincide with the (OCO). These values are in agreement with the expressions $0.5\theta_\ell+e$ and $0.5\theta_s-e$, in ref. 8 where θ_ℓ=27.96 mrad, and θ_s=23.5 mrad are the nominal bending angles of the long (Type A,C) and short (Type B) AGS magnets respectively and e = 2.138 mrad is an angle defined in ref. 8.

f) An optimization routine, which optimizes the strength of the bumps and the trim bumps, has been added to the code. This adjustment of the bump strength is necessary in order to achieve the proper excursion of the central orbit at the midpoint of straight sections G10 and H10 where the kicker and the extraction septum are located. In addition, this routine also adjusts (if needed) the bumps strengths for minimal residual oscillations of the equilibrium orbit.

TABLE A3.1
LOCATION OF THE AGS NEW EXTRACTION BUMPS

MAG #	MAG NAME	MAG TYPE	EFFECTIVE LENGTH (inches)	BACKLEG TURNS	MAXIMUM KICK (mrad)	$\Delta\theta/\theta 0$	POWER SUPPLY
108	F08	C	94	5	-0.99156	0.035457	1A
109	F09	B	79	6	-1.0	0.042550	1A
122	G02	B	79	6	-1.0	0.042550	1A
123	G03	C	94	5	-0.99156	0.035457	1A
130	G10	B	79	6	1.0	0.042550	1T
131	G11	B	79	6	1.0	0.042550	1T
136	G16	A	94	10	2.0	0.71518	1B
137	G17	C	94	10	2.0	0.71518	1B
144	H04	C	94	10	1.6	0.057214	2A
145	H05	A	94	10	1.6	0.057214	2A
148	H08	C	94	5	-0.99156	0.035457	2T
149	H09	B	79	6	-1.0	0.042550	2T
158	H18	C	94	5	-0.79325	0.028366	2B
159	H19	B	79	6	-0.8	0.034039	2B
172	I12	B	79	6	-0.8	0.034039	2B
173	I13	C	90	5	-0.79325	0.028366	2B

Table A3.1 Locations of the New Extraction Bump Coils. The extraction bump coils are backleg windings on AGS magnets listed on the first two columns of the table.